https://doi.org/10.5194/egusphere-2026-4405
Preprint. Discussion started: 28 September 2026

High-precision gravimetric primary standards for atmospheric Ar/N_2 measurements and redetermination of atmospheric Ar abundance

Nobuyuki Aoki[1,3,2], Shigeyuki Ishidoya[2,4,1], and Nobuhiro Matsumoto[3]

[1]Integrated Research Center for Nature Positive Technology, National Institute of Advanced Industrial Science and Technology, Tsukuba, Ibaraki 305-8567, Japan
[2]Global Zero Emission Research Center, National Institute of Advanced Industrial Science and Technology (GZR/AIST), Tsukuba 305-8569, Japan
[3]National Metrology Institute of Japan, National Institute of Advanced Industrial Science and Technology (NMIJ/AIST), Tsukuba 305-8563, Japan
[4]Research Institute for Environmental Management Technology, National Institute of Advanced Industrial Science and Technology (EMRI/AIST), Tsukuba 305-8569, Japan

Correspondence to: Nobuyuki Aoki (aoki-nobu@aist.go.jp)

Abstract. Accurate determination of atmospheric Ar/N_2 ratios requires primary standard gases with well-characterized uncertainties. However, an initial preparation approach based on the transfer of premixed gases introduced systematic deviations caused by transfer-induced composition changes, which limited the achievable accuracy. In this study, we developed an improved gravimetric preparation method for highly precise Ar standards (HPAs), in which CO_2, Ar, O_2, and N_2 are introduced independently from source gases. This approach eliminates transfer-induced compositional changes and allows the Ar amount to be determined directly with high precision. The resulting uncertainty in Ar/N_2 was reduced to approximately 5 per meg, corresponding to an Ar molar fraction of 0.05 μmol mol^{-1}. Validation confirmed that the gravimetric and measured values for CO_2, O_2/N_2, and Ar/N_2 agreed within their uncertainties. Using the validated HPAs, the absolute Ar/N_2 ratio of the AIST reference air was redetermined as 0.01195567 ± 0.000000011, a 8-fold reduction in uncertainty relative to the previous value. Application to atmospheric observations yielded an absolute Ar/N_2 ratio of 0.01195497 ± 0.00000013 and an Ar mole fraction of 9335.71 ± 0.10 μmol mol^{-1} in 2021. The numbers following the symbol ± represent the standard uncertainty. These results establish a metrologically traceable framework for high-precision atmospheric Ar measurements.

1 Introduction

The ocean plays a major role in regulating Earth's climate (Schuckmann et al., 2020 and 2023), absorbing and storing approximately 90 % of the excess heat that accumulates in the Earth system from greenhouse gas forcing (Rhein et al., 2013). This excess heat can be estimated from ocean heat content (OHC; Abraham et al., 2013), which is derived from ocean temperature measurements obtained by Argo floats (e.g., Cheng et al., 2019). Although substantial advances have been made, continuing efforts to expand deep-ocean coverage and reduce regional sampling biases are steadily improving the reliability of long-term OHC trend estimates.

The atmospheric Ar/N_2 ratio is a unique tracer for detecting changes in spatiotemporally integrated air–sea heat fluxes and ocean heat content. Variations in the Ar/N_2 ratio at the Earth's surface are driven by air–sea Ar and N_2 fluxes that reflect changes in gas solubility in seawater (e.g., Keeling et al., 2004). Integrated atmospheric Ar/N_2 ratios increase primarily because ocean warming reduces the solubility of Ar and N_2, with a larger relative response for Ar. The long-term trend in the atmospheric Ar/N_2 ratio can therefore provide an independent constraint on OHC estimates derived from ocean observations. To date, however, this trend has been reported only by Ishidoya et al. (2021), owing to the difficulty of achieving sufficient measurement accuracy, although several

https://doi.org/10.5194/egusphere-2026-4405
Preprint. Discussion started: 28 September 2026

studies have documented seasonal variations (Keeling et al., 2004; Blaine, 2005; Cassar et al., 2008; Ishidoya and Murayama, 2014).

At present, the application of atmospheric Ar/N_2 observations to OHC estimation is limited by the absence of highly precise Ar standard mixtures (HPAs) that can provide a common, metrologically traceable calibration scale. Hereafter, HPA refers to a standard gas mixture whose component molar fractions and associated uncertainties are well-defined and sufficiently small for atmospheric Ar/N_2 observation. As a result, individual laboratories have calibrated their measured Ar/N_2 values against their own reference air, whose absolute Ar/N_2 ratios are generally not known with sufficient uncertainty. The relative stability of the reference air can be evaluated through intercomparison with other air mixtures within a laboratory (e.g., Keeling et al., 2004; Ishidoya and Murayama, 2014), but its absolute stability cannot be verified. Furthermore, without HPAs, atmospheric Ar/N_2 observations can be expressed only on arbitrary scales, which prevents direct determination of absolute atmospheric Ar/N_2 ratios and limits comparability among observation networks. This limitation is particularly critical for OHC studies because the expected atmospheric variation is extremely small. Establishing a preparation method for HPAs with well-defined absolute Ar/N_2 ratios is therefore essential for improving the traceability, comparability, and long-term stability of atmospheric Ar/N_2 observations.

In a previous study, we developed highly precise O_2 standard mixtures (HPOs) containing N_2, O_2, Ar, and CO_2, with standard uncertainties of approximately 0.7 μmol mol^{-1} for Ar and 0.8 μmol mol^{-1} for N_2 (Aoki et al., 2019). These mixtures represented the most precise Ar/N_2 ratio reported to date. However, the corresponding uncertainty in the Ar/N_2 ratio was an order of magnitude larger than the analytical uncertainty of atmospheric Ar/N_2 measurements (Ishidoya et al., 2021; Keeling et al., 2004). The uncertainty of the standard mixture, rather than that of the analytical system, therefore became the dominant limitation on calibration accuracy. This uncertainty originated mainly from the gravimetric determination of the Ar amount introduced into the mixtures. Establishing a calibration scale suitable for long-term atmospheric Ar/N_2 observations therefore requires a substantial reduction in the uncertainty of the Ar molar fraction.

In this study, we address this limitation by developing a gravimetric preparation method designed specifically to improve the determination of the absolute Ar amount in HPAs. The resulting HPAs provide well-characterized absolute Ar/N_2 ratios with substantially improved uncertainty relative to previous standards. The molar fractions of the components in the HPAs were validated through measurements of the Ar/N_2, O_2/N_2, and CO_2 molar fractions. The HPAs were then applied to determine atmospheric Ar/N_2 ratios and Ar molar fractions in air samples. This study therefore establishes a metrologically traceable calibration framework for atmospheric Ar/N_2 observations, enabling the determination of absolute atmospheric Ar/N_2 ratios and providing a basis for improved long-term constraints on ocean heat uptake.

2 Materials and Methods

2.1 Preparation procedure

A total of eight HPAs were prepared by sequentially introducing pure CO_2, Ar, O_2, and N_2, in that order, into a 10 L aluminum alloy cylinder (Luxfer Gas Cylinders, UK). The cylinder was equipped with diaphragm valves (G-55, Hamai Industries Limited, Japan) sealed with poly(chlorotrifluoroethylene) (PCTFE). Preparation followed the procedure illustrated in Fig. 1 and was carried out in accordance with ISO 6142-1:2015. In this procedure, 0.9 L aluminum alloy cylinders, each fitted with a diaphragm valve connected by threaded fittings for Scotty transportable gas (SCOTTY 110, Air Liquide America Specialty Gases LLC), were used to accurately determine the masses of pure CO_2 and pure Ar transferred into the 10 L cylinder. First, using the filling system illustrated in Fig. 2(a), separate 0.9 L cylinders that had been evacuated to approximately 5.0×10^{-5} Pa were filled with pure CO_2 to 0.04 MPa and pure Ar to 1 MPa. The 10 L cylinder was evacuated to approximately 2.0×10^{-4} Pa with a turbomolecular pump

https://doi.org/10.5194/egusphere-2026-4405
Preprint. Discussion started: 28 September 2026

and weighed before filling. Using the transfer system illustrated in Fig. 2(b), pure CO_2 was then transferred from its 0.9 L cylinder into the 10 L cylinder, followed by pure Ar. Pure O_2 was introduced next, and the 10 L cylinder was weighed again. Finally, pure N_2 was added, and the cylinder was weighed once more.

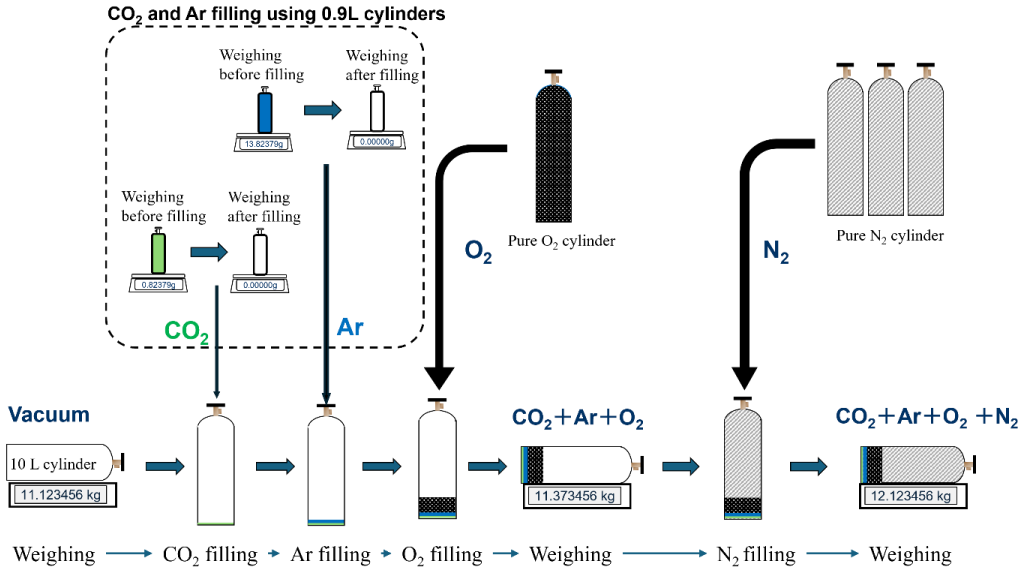

Figure 1. Preparation procedure for the highly precise Ar standard mixtures (HPAs).

The transferred and filled masses of CO_2, Ar, O_2, and N_2 were determined gravimetrically from the cylinder mass differences measured before and after each transfer or filling step. For CO_2 and Ar, the transferred masses, m_{CO_2} and m_{Ar}, were obtained from the mass loss of the 0.9 L cylinders. For O_2 and N_2, the filled masses, m_{O_2} and m_{N_2}, were determined from the mass increase of the 10 L sample cylinder.

$$m_{CO_2} = m_{0.9\,L,\ \text{before } CO_2 \text{ transfer}} - m_{0.9\,L,\ \text{after } CO_2 \text{ transfer}} \quad (1)$$

$$m_{Ar} = m_{0.9\,L,\ \text{before Ar transfer}} - m_{0.9\,L,\text{after Ar transfer}} \quad (2)$$

$$m_{O_2} = m_{10\,L,\ \text{after } O_2 \text{ filling}} - m_{10\,L,\ \text{vacuum}} - \left(m_{Ar} + m_{CO_2}\right) \quad (3)$$

$$m_{N_2} = m_{10\,L,\text{after } N_2 \text{ filling}} - m_{10\,L,\ \text{after } O_2 \text{ filling}} \quad (4)$$

Here $m_{0.9\,L,\ \text{before transfer}}$ and $m_{0.9\,L,\ \text{after transfer}}$ denote the masses of the 0.9 L sample cylinder immediately before and after transfer of the target gas to the 10 L sample cylinder, respectively. Likewise, $m_{10\,L,\ \text{vacuum}}$, $m_{10\,L,\ \text{afterafter } O_2 \text{ filling}}$, and $m_{10\,L,\ \text{afterafter } N_2 \text{ filling}}$ denote the masses of the 10 L sample cylinder in vacuum and the masses of the 10 L sample cylinder immediately after O_2 and N_2 filling steps, respectively. The standard uncertainty associated with each mass was obtained by combining the uncertainties of the individual values.

CO_2 and Ar remaining in the piping after transfer were driven into the 10 L cylinder by repeated pressurization–expansion cycles using pure O_2, as illustrated in Fig. 2(b). This flushing procedure was performed 100 times for CO_2 and 200 times for Ar. Based on the dilution factor of a single cycle, the residual fraction after these cycles was estimated to be negligible relative to the transferred amount. Pure O_2 and pure N_2 were filled into the 10 L cylinders using the same procedure reported previously for a

https://doi.org/10.5194/egusphere-2026-4405
Preprint. Discussion started: 28 September 2026

HPO (Aoki et al., 2019). The final pressure in the 10 L cylinder was approximately 9 MPa. Typical masses of the individual source gases were approximately 0.7 g for CO_2, 14 g for Ar, 250 g for O_2, and 800 g for N_2.

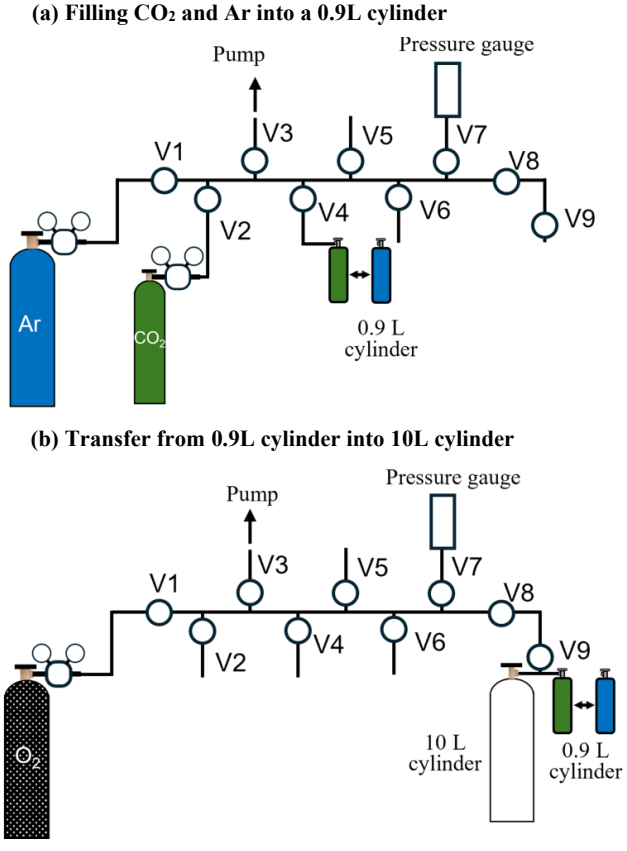

Filling procedure

1. Open V1 or V2, then open V4 and V7, and close the other valves.
2. Open V3 and evacuate the piping.
3. Close V3 and pressurize the piping with pure Ar or CO_2.
4. Open V3 and evacuate the piping.
5. Repeat the pressurization–evacuation cycle three times to condition the system.
6. Close V3 and pressurize the piping again with Ar or CO_2.
7. Open the valve of the 0.9 L cylinder, allowing the gas to expand into the 0.9 L cylinder.
8. Close the valve of the 0.9 L cylinder after filling.

Transfer procedure

1. Open V1, V7, V8, and V9, close the other valves, and open V3 to evacuate the piping.
2. Close V3 and pressurize the piping with O_2.
3. Open V3 and evacuate the piping.
4. Repeat the pressurization–evacuation cycle three times.
5. Close V3 and V9, then open the valves of the 0.9 L and 10 L cylinders (via V1) to transfer Ar or CO_2 into the 0.9 L cylinder.
6. Close the valves of both cylinders after transfer.
7. Open V9, then pressurize the piping with O_2, and immediately close V9.
8. Open the valve of the 10 L cylinder to allow O_2 to expand into the cylinder and then close the valve.
9. Repeat the pressurization–expansion cycle as required to ensure transfer of any residual gas.

Figure 2. Schematic of the filling system for (a) filling pure CO_2 and pure Ar into a 0.9 L cylinder and (b) transferring pure CO_2 and pure Ar from the 0.9 L cylinder into a 10 L cylinder.

2.2 Source gases and impurity analysis

Pure CO_2 (>99.998 %, Nippon Ekitan Corporation, Japan), pure Ar (G1 grade, 99.9999 %, Japan Fine Products, Japan), pure O_2 (G1 grade, 99.99995 %, Japan Fine Products, Japan), and pure N_2 (G1 grade, 99.99995 %, Japan Fine Products, Japan) were used as source gases for preparation of the HPAs. Impurities in the source gases were identified and quantified using several analytical techniques. The molar fractions of the impurities N_2, O_2, CH_4, and H_2 in pure CO_2, Ar in pure N_2, and N_2 in pure O_2 were determined by gas chromatography–thermal conductivity detection (GC–TCD). A Fourier transform infrared spectrometer was used to detect impurity CO_2, CH_4, and CO in pure N_2, O_2, and Ar. Impurity O_2 in pure N_2 and Ar was quantified using a galvanic-cell-type O_2

https://doi.org/10.5194/egusphere-2026-4405
Preprint. Discussion started: 28 September 2026

analyzer. Impurity water (H_2O) in pure CO_2 was measured with a capacitance-type moisture meter, whereas H_2O in pure N_2, O_2, and Ar was measured using a cavity ring-down-spectrometer-based moisture analyzer.

2.3 Weighing procedure

The 0.9 L cylinders were weighed using a custom-built weighing system, and the 10 L cylinder was weighed using the system developed by Matsumoto et al. (2004). In this study, a cylinder whose mass was measured is hereafter referred to as a "sample cylinder." Each sample cylinder was weighed relative to an almost identical reference cylinder to minimize the effects of mass comparator drift, sensitivity variations, buoyancy changes, and surface adsorption of water vapor (Alink et al., 2000; Milton et al., 2011). The mass difference between the sample and reference cylinders was used as the mass reading.

2.3.1 Weighing of a 0.9 L cylinder

The custom-built weighing system consists of a mass comparator (AX2005, Mettler Toledo, Switzerland) and an automated cylinder transfer device, as shown in Fig. 3. The mass comparator had a maximum capacity of 2.1 kg, a sensitivity of 0.01 mg, and a linearity of 0.04 mg. The transfer device comprised two compact actuators (SKR3306B and SKR2602B, THK Co., Ltd., Japan), a ball spline bearing with a rolling guide (LBG20, THK Co., Ltd., Japan), two stepper motors (ARM46, Oriental Motor Co., Ltd., Japan), an aluminum arm (Fujikin Incorporated, Japan), and two cylinder holders (Fujikin Incorporated, Japan). The entire weighing system was enclosed within an acrylic draft shield to minimize the influence of ambient air convection, and the stepper motors were positioned outside the enclosure to further reduce thermal disturbances.

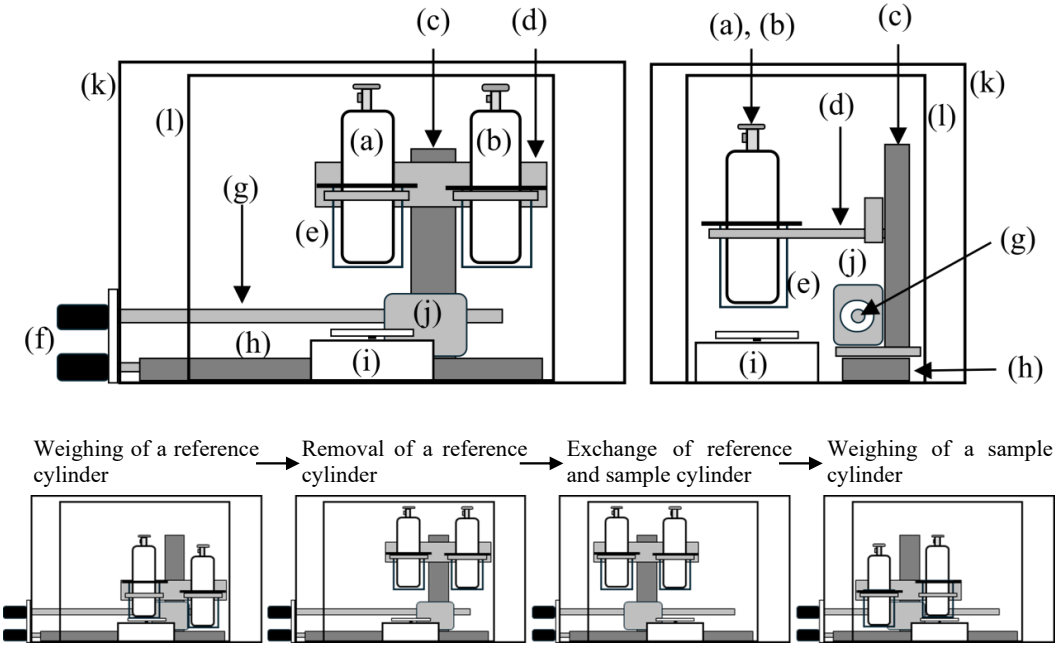

Figure 3. Schematic of the weighing system used to determine the masses of pure Ar and pure CO_2 to be filled: (a) sample cylinder, (b) reference cylinder, (c) linear actuator for vertical transfer, (d) Al-base arm, (e) Al-base cylinder holder, (f) motor, (g) ball spline, (h) linear actuator for horizontal transfer, (i) electronic mass comparator, (j) gearbox, (k) windshield panel, and (l) windshield panel.

https://doi.org/10.5194/egusphere-2026-4405
Preprint. Discussion started: 28 September 2026

All mass measurements were performed in a temperature- and humidity-controlled room maintained at 25 ± 0.5°C and 50 ± 1 %, respectively. The ambient temperature and humidity in the acrylic draft shield were continuously monitored using a USB-connected data logger (TR-73, T&D Corporation, Japan), and atmospheric pressure was measured using a pressure sensor (Druck RPS DPS 8100 TERPS Pressure Sensor, Baker Hughes Company, USA). Mass measurements followed an ABBA sequence (reference–sample–sample–reference), where "A" and "B" represent the reference and sample cylinders, respectively. Loading and unloading of the cylinders were fully automated, and one complete ABBA cycle required approximately 6 min. The mass reading, obtained from the mass comparator readings within each ABBA cycle, was used to determine the relative mass of the sample cylinder.

The masses of pure CO_2 and Ar were then determined from the difference in the mass readings before and after gas transfer.

2.3.2 Weighing of a 10 L cylinder

This weighing system consists of a mass comparator (XP26003L, Mettler Toledo, Switzerland) and an automated cylinder transfer device. The comparator had a maximum capacity of 26.1 kg, a sensitivity of 1 mg, and a linearity of 20 mg. All mass measurements were conducted in the same weighing room described in Section 2.3.1, and ambient temperature, humidity, and atmospheric pressure were continuously monitored using the TR-73 data logger.

Detailed procedures for weighing the 10 L cylinders have been described elsewhere (Aoki et al., 2019) and are therefore only briefly summarized here. The sample cylinder was weighed relative to an almost identical reference cylinder in an ABBA sequence. Measurements began once the temperature difference between the sample and reference cylinders, checked with a thermocouple thermometer, had become negligible.

2.3.3 Determination of cylinder volume expansion

Pressure-dependent cylinder expansion was evaluated because changes in cylinder volume affect the buoyancy correction applied to mass measurements. Consequently, cylinder expansion contributes to the uncertainty of the Ar molar fraction. The volume expansion of the 0.9 L and 10 L cylinders under internal pressure was determined by measuring changes in water volume during controlled depressurization using the method described by Oh et al. (2013). The experimental setup is illustrated schematically in Fig. 4. The results are presented in the section 4.1.2.

Each test cylinder was filled with pure N_2 and pressurized to 12 MPa. The cylinder was then placed in a water bath filled completely with deionized water, leaving no headspace. The water bath for the 0.9 L cylinder was made of acrylic resin (volume: approximately 8.8 dm^3; radius: 7.5 cm; height: 50 cm), whereas that for the 10 L cylinder was constructed from stainless steel (volume: approximately 61 dm^3; radius: 15.5 cm; height: 81 cm). The cylinder was connected to a vent line through stainless-steel tubing with an inner diameter of 1.59 mm, and a vertical volumetric pipette was mounted at the top of the bath to monitor water displacement. Pipettes with capacities of 2 mL and 25 mL (custom A, 2ML and 25ML, SIBATA SCIENTIFIC TECHNOLOGY LTD., Japan) were used for the 0.9 L and 10 L cylinders, respectively. The initial water level was set to an arbitrarily determined reference zero position, and the external volume change of the cylinder was assumed to equal the displaced water volume measured in the pipette.

After thermal equilibrium was established, the internal gas pressure in the cylinder was gradually reduced by venting gas through the regulator. During depressurization, changes in the water level in the volumetric pipette were recorded at pressure intervals of

https://doi.org/10.5194/egusphere-2026-4405
Preprint. Discussion started: 28 September 2026

2 MPa. The change in water volume associated with depressurization was used to quantify the pressure-dependent expansion of the cylinder.

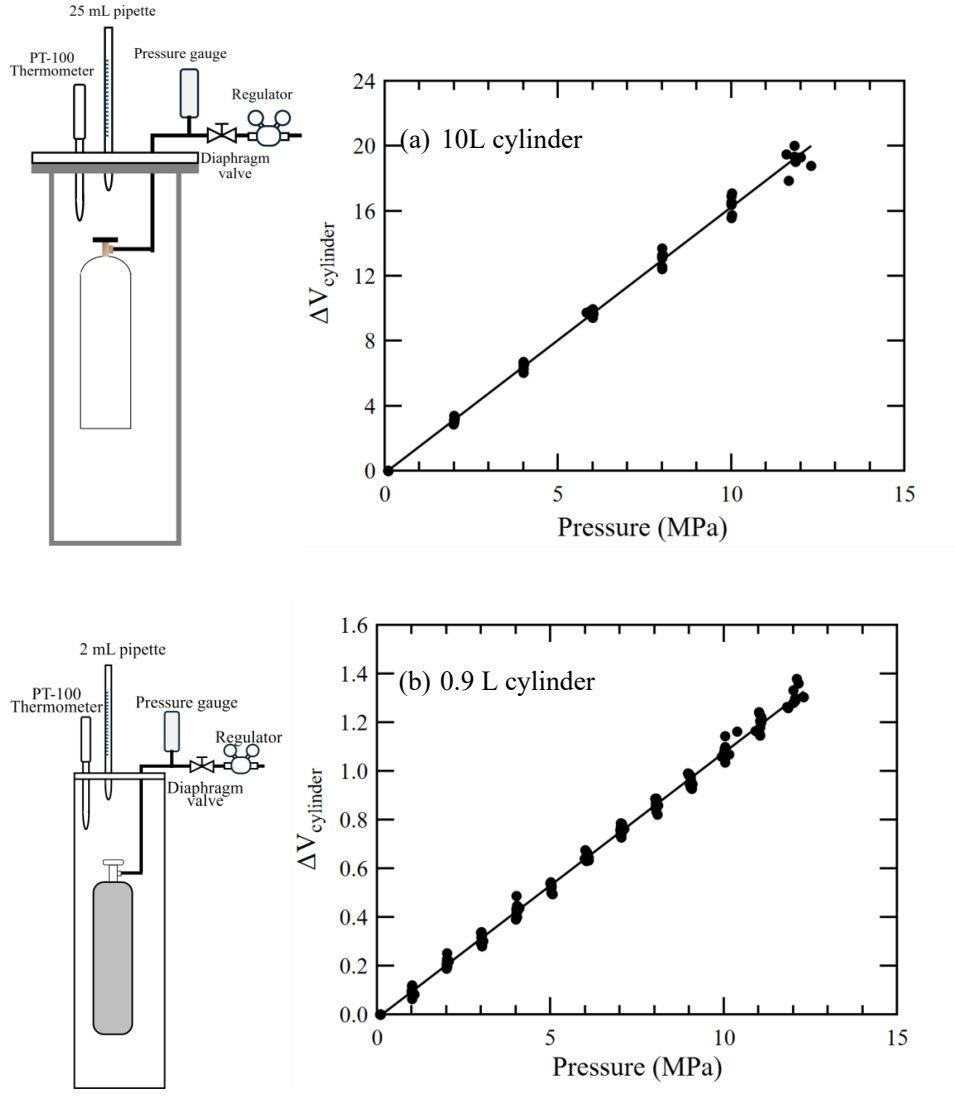

Figure 4. Experimental setup and results of indirect measurements of changes in external cylinder volume for (a) a 10 L aluminum cylinder and (b) a 0.9 L aluminum cylinder during continuous gas release from 12 MPa to 0.1 MPa.

160 The internal gas pressure was monitored using a pressure transducer (PPA-33X, KELLER AG, Switzerland) and a digital indicator (EV-120, KELLER AG, Switzerland). Water temperature was measured simultaneously using a platinum resistance thermometer (Pt100, Chino Corporation, Japan).

https://doi.org/10.5194/egusphere-2026-4405
Preprint. Discussion started: 28 September 2026

2.4 Determination of molar masses of Ar, O_2, and N_2

The molar fractions of the constituents in each HPA were calculated from the amount of substance of each source gas. Accurate determination of this amount in the 10 L cylinder requires knowledge of both the filling mass and the molar mass of the respective source gas, and the molar masses were calculated from the isotopic composition of the source gases.

The isotopic compositions of Ar, O_2, and N_2 may vary among the HPAs and were therefore determined by measuring the isotope ratios of Ar, O_2, and N_2 in the HPAs. Because the HPAs were prepared by directly mixing source gases from one cylinder of pure Ar, one cylinder of pure O_2, and three or four cylinders of pure N_2, the isotopic compositions of the source gases were assumed to correspond to those of the components in the HPAs. The isotopic composition of the source gases can therefore be inferred from the measured isotope ratios.

Because the analytical procedures for the O_2 and N_2 isotope ratios were identical to those described previously (Aoki et al., 2019), only the procedure for Ar is summarized here. The isotopic abundances of ^{36}Ar, ^{38}Ar, and ^{40}Ar in the source gases were inferred from isotope ratio measurements of the HPAs. The $^{36}Ar/^{40}Ar$ ratio was calculated as $^{36}Ar/^{40}Ar = [\delta(^{36}Ar/^{40}Ar) + 1] \times (^{36}Ar/^{40}Ar)_{ref}$, where the $\delta(^{36}Ar/^{40}Ar)$ values were determined using a stable isotope ratio mass spectrometer (Delta V, Thermo Fisher Scientific, USA). This value represents the deviation from the atmospheric reference composition, as natural air was used as the reference material (Ishidoya and Murayama, 2014). The ^{38}Ar isotope could not be measured directly by the mass spectrometer; therefore, the ^{38}Ar abundance was assumed to equal the atmospheric value (0.0006289; Böhlke, 2014). The associated standard uncertainty was conservatively estimated from the deviation of the $^{36}Ar/^{40}Ar$ ratio from the atmospheric value observed in pure Ar, because the $^{36}Ar/^{40}Ar$ ratio is more sensitive to isotopic variations than the $^{38}Ar/^{40}Ar$ ratio.

2.5 Analytical validations

2.5.1 Ar/N_2 and O_2/N_2 ratios

The Ar/N_2 and O_2/N_2 ratios in the HPAs were measured using a newly introduced stable isotope mass spectrometer (Delta Q, Thermo Fisher Scientific, USA) and the conventional stable isotope ratio mass spectrometer (Delta V, Thermo Fisher Scientific, USA) used in our previous study. The measurement procedure for the conventional mass spectrometer has been described elsewhere (Ishidoya and Murayama, 2014). The procedure for the new mass spectrometer will be reported elsewhere, but the method used to measure the standard gases is, in principle, the same as that for the conventional mass spectrometer.

Atmospheric Ar/N_2 and O_2/N_2 ratios are commonly expressed relative to an arbitrary reference gas in per meg units (Keeling and Shertz, 1992; Keeling et al., 2004).

$$\delta(\mathrm{Ar/N_2}) = \left(\frac{[n(\mathrm{Ar})/n(\mathrm{N_2})]_{\mathrm{sam}}}{[n(\mathrm{Ar})/n(\mathrm{N_2})]_{\mathrm{ref}}} - 1\right) \times 10^6 \quad (5)$$

$$\delta(\mathrm{O_2/N_2}) = \left(\frac{[n(\mathrm{O_2})/n(\mathrm{N_2})]_{\mathrm{sam}}}{[n(\mathrm{O_2})/n(\mathrm{N_2})]_{\mathrm{ref}}} - 1\right) \times 10^6 \quad (6)$$

Here, n denotes the amount of each substance, and the subscripts "sam" and "ref" refer to sample air and reference air, respectively. Because the atmospheric molar fractions of O_2 and Ar are 209339 μmol mol^{-1} and 9334 μmol mol^{-1}, respectively (Aoki et al., 2019), 5 per meg of $\delta(O_2/N_2)$ and $\delta(Ar/N_2)$ corresponds to 1 μmol mol^{-1} and 0.05 μmol mol^{-1}, respectively. In this study, AIST reference air was used as the reference gas, and all values reported on the EMRI/AIST scale are referenced to this air.

https://doi.org/10.5194/egusphere-2026-4405
Preprint. Discussion started: 28 September 2026

The mass spectrometers were configured to simultaneously measure ion beam currents at mass-to-charge ratios of 28 ($^{14}N^{14}N$), 29 ($^{15}N^{14}N$), 32 ($^{16}O^{16}O$), 33 ($^{17}O^{16}O$), 34 ($^{18}O^{16}O$), 36 (^{36}Ar), 40 (^{40}Ar), and 44 ($^{12}C^{16}O^{16}O$). The isotopic ratios $\delta(^{15}N^{14}N/^{14}N^{14}N)$, $\delta(^{17}O^{16}O/^{16}O^{16}O)$, $\delta(^{18}O^{16}O/^{16}O^{16}O)$, $\delta(^{16}O^{16}O/^{14}N^{14}N)$, $\delta(^{36}Ar/^{40}Ar)$, and $\delta(^{40}Ar/^{14}N^{14}N)$ were determined relative to the AIST reference air. Because the isotopic compositions of the source gases differed from atmospheric values, the gravimetrically calculated ratios $\delta(O_2/N_2)_{HPA\_grav}$ and $\delta(Ar/N_2)_{HPA\_grav}$ did not correspond directly to the measured isotopic ratios $\delta(^{16}O^{16}O/^{14}N^{14}N)_{HPA\_meas}$ and $\delta(^{40}Ar/^{14}N^{14}N)_{HPA\_meas}$. Hereafter, the subscripts "HPA_grav" and "HPA_meas" denote gravimetric and measured values, respectively.

The values $\delta(O_2/N_2)_{HPA\_meas}$ and $\delta(Ar/N_2)_{HPA\_meas}$ were calculated using equations (7) and (8) from the measured isotope ratios $^{15}N^{14}N/^{14}N^{14}N$, $^{17}O^{16}O/^{16}O^{16}O$, $^{18}O^{16}O/^{16}O^{16}O$, $^{36}Ar/^{40}Ar$, and $^{38}Ar/^{40}Ar$. Isotopologues such as $^{17}O^{17}O$, $^{18}O^{17}O$, $^{18}O^{18}O$, and $^{15}N^{15}N$ were neglected because of their extremely low abundances.

$$\delta(O_2/N_2)_{HPA\_meas} = \left[\delta(^{16}O^{16}O/\,^{14}N\,^{14}N)_{HPA\_meas} + 1\right] \times \left[\frac{1+^{17}O^{16}O/^{16}O^{16}O+^{18}O^{16}O/^{16}O^{16}O}{1+^{15}N\,^{14}N/^{14}N^{14}N}\right]_{HPA} \Big/ \left[\frac{1+^{17}O^{16}O/^{16}O^{16}O+^{18}O^{16}O/^{16}O^{16}O}{1+^{15}N\,^{14}N/^{14}N\,^{14}N}\right]_{ref} - 1 \quad (7)$$

$$\delta(Ar/N_2)_{HPA\_meas} = \left[\delta(^{40}Ar/\,^{14}N^{14}N)_{HPA\_meas} + 1\right] \times \left[\frac{1+^{36}Ar/^{40}Ar+^{38}Ar/^{40}Ar}{1+^{15}N\,^{14}N/^{14}N^{14}N}\right]_{HPA} \Big/ \left[\frac{1+^{36}Ar/^{40}Ar+^{38}Ar/^{40}Ar}{1+^{15}N\,^{14}N/^{14}N^{14}N}\right]_{ref} - 1 \quad (8)$$

2.5.2 CO_2 analysis

The molar fractions of CO_2 in the HPAs were measured using a cavity ring-down spectrometer (G2301, Picarro Inc., USA) equipped with a multi-port inlet valve (Valco Instruments Co. Inc., USA) and a mass flow controller (SEC-N112, Horiba STEC, Japan). The instrument was calibrated using three to five primary standard gases gravimetrically prepared with CO_2 molar fractions of 330 μmol mol^{-1} to 500 μmol mol^{-1}. These standards were prepared from pure CO_2 and purified air in accordance with ISO 6142-1:2015 and are traceable to SI units; their associated standard uncertainties were approximately 0.80 μmol mol^{-1}. Each standard gas was measured continuously at a flow rate of 80 mL min^{-1} for 20 min, and data from the final 10 min were used to ensure signal stabilization. The calibration range covered the molar fraction range of the measured HPAs.

The same source CO_2 gas used in preparing the HPAs was used to prepare the calibration gases, ensuring consistency in isotopic composition.

3 Preparation of Standard Mixtures

3.1 Initial preparation approach and expected uncertainty

The HPOs developed in our previous study were prepared by sequentially filling a 10 L cylinder with source gases, including a premixed CO_2/Ar gas, O_2, and N_2 (Aoki et al., 2019). The standard uncertainties of the $\delta(Ar/N_2)$ values in these mixtures were approximately 70 per meg, corresponding to about 0.7 μmol mol^{-1} for the Ar molar fraction.

The uncertainty budget analysis indicated that the dominant contributors to the uncertainty of the Ar molar fraction were the determinations of the CO_2/Ar filling mass and the Ar molar mass. In addition, the Ar detected as an impurity in pure N_2 cannot be neglected at the uncertainty level required for HPAs, so accurate and traceable quantification of Ar in pure N_2 is also essential. In

https://doi.org/10.5194/egusphere-2026-4405
Preprint. Discussion started: 28 September 2026

contrast, the standard uncertainty of the atmospheric Ar/N_2 ratio measurement is 3 per meg to 7 per meg (Ishidoya et al., 2021; Birner et al., 2020), which corresponds to 0.03 μmol mol^{-1} to 0.07 μmol mol^{-1} for the Ar molar fraction. The target standard uncertainty for the Ar/N_2 ratio was therefore set to ≤7 per meg, comparable to the measurement uncertainty of the analytical system used for atmospheric observations. In this study, we first improved the preparation procedure to reduce the dominant uncertainty associated with determination of the Ar filling mass (Sections 3.1–3.3). We then addressed the remaining major uncertainty sources, namely Ar impurities in pure N_2 and the molar mass of Ar.

3.2 Evaluation of the initial preparation procedure

To reduce the uncertainty associated with the CO_2/Ar mass, an alternative procedure was implemented in which the CO_2/Ar mixture was first filled into the 0.9 L cylinder and then transferred into a 10 L cylinder. In this procedure, the mass of the CO_2/Ar mixture was determined from the mass loss of the 0.9 L cylinder before and after transfer. In contrast, O_2 and N_2 were filled directly into the 10 L cylinder using the same procedure as for the HPOs. The gravimetrically calculated standard uncertainty of the Ar molar fraction in HPAs prepared by this procedure was estimated to be 0.05 μmol mol^{-1}, indicating that the target uncertainty should have been achieved. No significant discrepancy between the gravimetric and analytical values was therefore expected.

3.3 Identification and investigation of the discrepancy

Despite the low gravimetric uncertainty, substantial discrepancies were observed among lots prepared independently in different years (2020, 2022, and 2023), as well as among lots prepared in 2023 from different CO_2/Ar mixtures (CPB28687 and CPC00418). As shown in Fig. 5, systematic differences of approximately 100 per meg in $\delta(Ar/N_2)$ were observed among the lots. This discrepancy is more than two orders of magnitude larger than the annual atmospheric increase in Ar/N_2 (0.7 per meg to 0.9 per meg; Ishidoya et al., 2021) and is therefore incompatible with the requirements for long-term atmospheric Ar/N_2 observations. Furthermore, the slope of the relationship between the gravimetric and measured $\delta(Ar/N_2)$ values differed among the lots, by as much as 1.2 %. This indicates that the discrepancy affected not only the assigned values but also the calibration relationship itself. Such differences cannot be ignored for long-term, climate-related applications that require a highly stable reference.

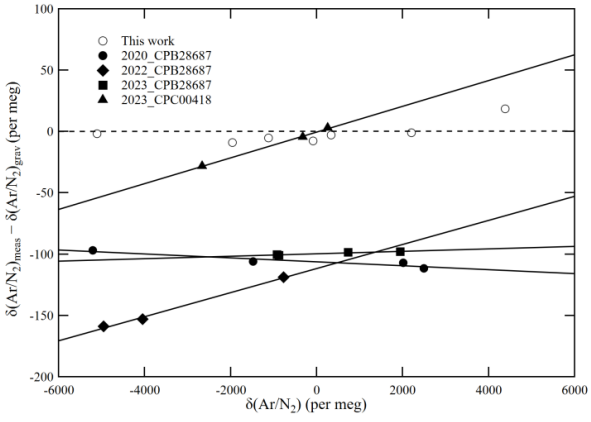

Figure 5. Differences between the gravimetrically assigned $\delta(Ar/N_2)$ values and the corresponding $\delta(Ar/N_2)$ values on the EMRI/AIST scale in standard mixtures prepared from CO_2/Ar, O_2, and N_2 source gases. Open circles represent the values for the HPAs developed in this study. Closed circles, diamonds, squares, and triangles represent the values for standard mixtures prepared from CO_2/Ar mixture CPB28687 in 2020, 2022, and 2023 and from CO_2/Ar mixture CPC00418 in 2023, respectively.

https://doi.org/10.5194/egusphere-2026-4405
Preprint. Discussion started: 28 September 2026

Several potential causes were considered: (i) long-term drift of the weighing system, (ii) residual CO_2/Ar mixture in the transfer lines, and (iii) compositional changes during transfer of the CO_2/Ar mixture. The weighing system was calibrated before each preparation using SI-traceable standard weights, which reduced the effect of long-term drift to a negligible level, and the residual CO_2/Ar mixture was fully transferred from the 0.9 L cylinder into the 10 L cylinder by repeated pressurization–expansion cycles. Previous transfer experiments using CO_2/Ar mixtures have demonstrated measurable compositional changes during cylinder-to-cylinder transfer (Aoki et al., 2022, 2025). Transfer-induced compositional changes were therefore considered the most likely explanation for the observed discrepancies.

3.4 Improved preparation procedure

Based on these findings, the preparation procedure used in Section 3.2 was judged unsuitable for producing HPAs. An alternative approach was therefore developed, in which CO_2, Ar, O_2, and N_2 were introduced independently from source gases, as illustrated in Fig. 1. By eliminating the transfer of premixed CO_2/Ar mixtures, the new procedure avoided the composition changes associated with mixture transfer.

In the developed procedure, pure CO_2 and Ar were first aliquoted into 0.9 L cylinders and then transferred to 10 L cylinders, and their transfer masses were determined precisely from the mass loss of the 0.9 L cylinders before and after each transfer using equations (1) and (2). Direct gravimetric determination of the Ar filling mass in the 10 L cylinder was not feasible because the required uncertainty was substantially smaller than the weighing uncertainty of the 10 L cylinder. The transferred Ar mass was therefore determined from the mass difference of the 0.9 L cylinder using the newly developed high-precision weighing system shown in Fig. 3.

Table 1. Gravimetric values of the N_2, O_2, Ar, and CO_2 molar fractions, together with $(O_2/N_2)_{HPA\_grav}$, $(Ar/N_2)_{HPA\_grav}$, $\delta(O_2/N_2)_{HPA\_grav}$, and $\delta(Ar/N_2)_{HPA\_grav}$, and the measured values of the CO_2 molar fractions in the HPAs.

Cylinder number	Preparation date	Gravimetric values[a]							
		N_2	O_2	Ar	CO_2	$(O_2/N_2)_{HPA\_grav}$	$(Ar/N_2)_{HPA\_grav}$	$\delta(O_2/N_2)_{HPA\_grav}$ [b]	$\delta(Ar/N_2)_{HPA\_grav}$ [c]
CPB12763	2024/4/25	781012.40 ± 0.74	209236.63 ± 0.74	9340.66 ± 0.05	410.14 ± 0.04	0.2679049 ± 0.0000010	0.01195968 ± 0.00000007	−701.3 ± 3.7	335.3 ± 5.8
CPB16187	2024/4/23	781104.69 ± 0.74	209113.87 ± 0.74	9379.60 ± 0.05	401.66 ± 0.04	0.2677155 ± 0.0000010	0.01200812 ± 0.00000007	−1407.5 ± 3.7	4386.9 ± 5.9
CPB16370	2024/5/1	781214.93 ± 0.73	209042.20 ± 0.74	9321.65 ± 0.05	421.04 ± 0.04	0.2675860 ± 0.0000010	0.01193225 ± 0.00000007	−1890.6 ± 3.6	−1959.4 ± 5.3
CPB31357	2024/8/20	780784.73 ± 0.74	209465.32 ± 0.74	9355.38 ± 0.05	394.40 ± 0.04	0.2682754 ± 0.0000010	0.01198202 ± 0.00000006	680.7 ± 3.7	2203.3 ± 5.3
CPB16246	2024/10/11	780341.66 ± 0.73	209899.28 ± 0.74	9328.74 ± 0.05	430.14 ± 0.04	0.2689838 ± 0.0000010	0.01195468 ± 0.00000006	3323.2 ± 3.6	−83.0 ± 5.3
CPC00484	2024/10/31	782125.75 ± 0.73	208184.25 ± 0.73	9251.35 ± 0.05	438.48 ± 0.04	0.2661775 ± 0.0000010	0.01182847 ± 0.00000007	−7144.7 ± 3.6	−10639.9 ± 5.6
CPB28571	2025/6/10	780402.28 ± 0.73	209867.83 ± 0.73	9319.79 ± 0.04	409.93 ± 0.04	0.2689230 ± 0.0000010	0.01194230 ± 0.00000006	3096.5 ± 3.6	−1119.1 ± 4.8
CPC00486	2025/6/19	781217.85 ± 0.73	209038.84 ± 0.76	9292.25 ± 0.05	450.88 ± 0.04	0.2675807 ± 0.0000010	0.01189457 ± 0.00000006	−1910.4 ± 3.8	−5110.7 ± 5.4

[a] Numbers following the symbol ± denote the standard uncertainty. Values for CO_2, Ar, O_2, and N_2 are given in μmol mol, and for $\delta(O_2/N_2)_{HPA\_grav}$ and $\delta(Ar/N_2)_{HPA\_grav}$ in per meg.

[b] Values were calculated using the absolute O_2/N_2 in the AIST reference air, as described in Aoki et al. (2019).

[c] Values were calculated using the absolute Ar/N_2 in the AIST reference air determined in Section 4.3.

https://doi.org/10.5194/egusphere-2026-4405
Preprint. Discussion started: 28 September 2026

https://doi.org/10.5194/egusphere-2026-4405
Preprint. Discussion started: 28 September 2026

4 Results

4.1 Calculation of molar fractions and uncertainties

The gravimetric molar fractions and their associated standard uncertainties for the HPAs are summarized in Table 1. The standard uncertainties were 0.7 μmol mol^{-1} for N_2, 0.7 μmol mol^{-1} for O_2, 0.05 μmol mol^{-1} for Ar, 0.04 μmol mol^{-1} for CO_2, and 4.8 per meg to 5.9 per meg for δ(Ar/N_2). The target uncertainty of ≤7 per meg was thus achieved. The gravimetric molar fraction (y_k) of constituent k (CO_2, Ar, O_2, or N_2) was calculated according to ISO 6142-1:2015.

$$y_k = \frac{\sum_{j=1}^{r}\left(\frac{x_{k,j}\times m_j}{\sum_{i=1}^{q} x_{i,j}\times M_i}\right)}{\sum_{j=1}^{r}\left(\frac{m_j}{\sum_{i=1}^{q} x_{i,j}\times M_i}\right)} \quad (9)$$

In this equation, (M_i), ($x_{i,j}$), and (m_j) represent the molar mass, the molar fraction of constituent *i* (CO_2, Ar, O_2, N_2, and impurities) in source gas *j* (pure CO_2, pure Ar, pure O_2, and pure N_2), and the mass of each source gas, respectively. *r* and *q* represent the number of source gases *j* and constituents *i*, respectively, and $x_{k,j}$ is the molar fraction of constituent *k* in source gas j.

The standard uncertainty ($u(y_k)$) associated with the gravimetric molar fraction was calculated using the law of propagation of uncertainty:

$$u^2(y_k) = \sum_{j=1}^{r}\sum_{i=1}^{q}\left(\frac{\partial y_k}{\partial x_{i,j}}\right)^2 \times u^2(x_{i,j}) + \sum_{i=1}^{q}\left(\frac{\partial y_k}{\partial M_i}\right)^2 \times u^2(M_i) + \sum_{j=1}^{r}\left(\frac{\partial y_k}{\partial m_j}\right)^2 \times u^2(m_j) \quad (10)$$

Here, $u(A)$ denotes the standard uncertainty associated with quantity A. Table 2 lists the contributions of the purity of the source gases, the molar masses of the constituents, and the masses of the source gases to the gravimetric molar fraction. These correspond to the square roots of the first, second, and third terms in equation (10), respectively. These contributions to the Ar molar fraction uncertainty arose mainly from the masses of the source gases and their purity. The contribution of the molar mass uncertainty was negligible. The purity of the individual source gases, the molar masses of the constituents i, and the masses of the source gases, together with their associated standard uncertainties, are described in Sections 4.1.1, 4.1.2, and 4.1.3.

Table 2. Typical contribution of each source of uncertainty (mass of the source gas, molar mass, and purity) to the standard uncertainties obtained for the molar fractions of N_2, O_2, Ar, and CO_2 in the HPAs.

Constituent	Uncertainty source, μmol mol^{-1}			Combined standard uncertainty, μmol mol^{-1}
	Mass of source gas [a]	Molar mass [b]	Purity [c]	
N_2	0.75	0.03	0.07	0.76
O_2	0.76	0.03	0.03	0.76
Ar	0.043	0.002	0.023	0.049
	Contribution	Contribution	Contribution	
	CO_2 0.000	CO_2 0.000	Ar in pure N_2 0.023	
	Ar 0.041	Ar 0.002	Ar in pure O_2 0.005	

https://doi.org/10.5194/egusphere-2026-4405
Preprint. Discussion started: 28 September 2026

	O_2 0.009 N_2 0.010	O_2 0.000 N_2 0.001	Other impurities < 0.001	
CO_2	0.032	0.006	0.001	0.032

[a] The values were calculated using the procedure described in Section 4.1.3.

[b] The values were calculated using the procedure described in Section 4.1.2.

[c] The values were calculated using the procedure described in Section 4.1.1.

4.1.1 Purity of source gas

The molar fractions of impurities and their associated standard uncertainties in each source gas were determined using dynamically prepared standard mixtures in accordance with ISO 6145-7. When the molar fraction of an impurity h was below its detection limit ($L_{h,j}$), the molar fraction ($x_{h,j}$) and its standard uncertainty ($u(x_{h,j})$) in source gas j were estimated as $x_{h,j} = L_{h,j}/2$ and $u(x_{h,j}) = L_{h,j}/2\sqrt{3}$. The calculated impurity molar fractions and the resulting purities of the source gases are summarized in Table 3. The purities of Ar and O_2 were greater than 99.9999 %, whereas CO_2 was 99.99949 % and N_2 ranged from 99.99936 % to 99.99998 %.

Table 3. Impurities in source gases used for preparation of the HPAs.

Impurity	Source gases, μmol mol^{-1}			
	CO_2	Ar	O_2	N_2
N_2	1.5 ± 0.9	0.10 ± 0.06	0.25 ± 0.14	N/A
O_2	0.85 ± 0.49	0.058 ± 0.001	N/A	0.025 ± 0.014
Ar	-	N/A	0.039 ± 0.023	0.046 ± 0.029, 0.145 ± 0.040 3.066 ± 0.032, 3.501 ± 0.020 6.250 ± 0.050
CO_2	N/A	0.002 ± 0.001	0.016 ± 0.003	0.002 ± 0.001
H_2O	1.30 ± 0.75	0.06 ± 0.03	0.27 ± 0.16	0.05 ± 0.03
CH_4	0.26 ± 0.01	0.005 ± 0.003	0.005 ± 0.003	0.005 ± 0.003
CO	0.20 ± 0.12	0.04 ± 0.02	0.04 ± 0.02	0.04 ± 0.02
H_2	0.85 ± 0.49	-	-	-
Purity	999994.9 ± 1.4	999999.73 ± 0.07	999999.38 ± 0.22	999999.82 ± 0.05, 999999.72 ± 0.06 999996.80 ± 0.05, 999996.37 ± 0.06 999993.62 ± 0.07,

Numbers following the symbol ± denote the standard uncertainty.

"-" indicates constituents that were not measured.

"N/A" indicates that the analyte is the major component of the source gas.

Among the identified impurities, Ar in pure N_2 was the dominant contributor to the uncertainty of the Ar molar fraction and therefore required particular attention, as shown in Table 2. Ar in pure N_2 was measured by GC–TCD. Quantification was performed relative to standard mixtures dynamically prepared from an Ar/He standard mixture (Ar molar fraction: 20.316 ± 0.035

https://doi.org/10.5194/egusphere-2026-4405
Preprint. Discussion started: 28 September 2026

μmol mol^{-1}) with pure He using mass flow controllers. The resulting Ar molar fractions in the calibration standard mixtures were 6.772 ± 0.030 μmol mol^{-1}, 3.694 ± 0.004 μmol mol^{-1}, 2.902 ± 0.011 μmol mol^{-1}, 1.741 ± 0.037 μmol mol^{-1}, and 0.580 ± 0.0014 μmol mol^{-1}. A molecular sieve 5A was used as the analytical column. The column temperature was maintained at 90°C, pure He was used as the carrier gas at a flow rate of 30 mL min^{-1}, and the total analysis time was 20 min per injection. A representative chromatogram is shown in Fig. 6.

In our chromatographic system, the Ar and O_2 peaks were detected as a single combined peak because they could not be separated under the conditions used. To prevent the major component (N_2) from degrading the quantification accuracy, N_2 was removed from the system using a valve-switching procedure. After elution of the Ar+O_2 peak, a valve was switched to vent N_2 out of the system and then returned to its original position. As shown in Fig. 6, the post-switch baseline returned to a level comparable to that before Ar+O_2 elution, indicating that N_2 was effectively purged and that the valve-switching operation introduced no measurable baseline drift.

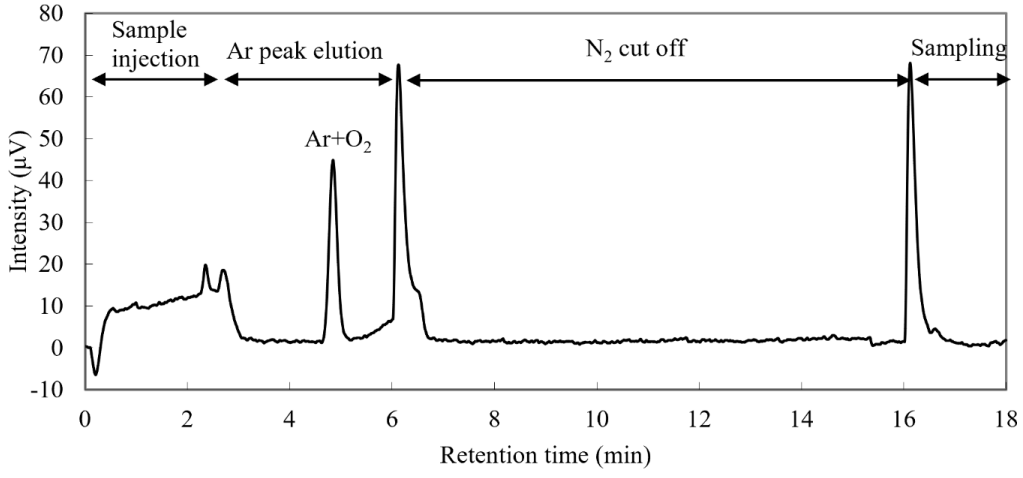

Figure 6. Chromatogram obtained from the measurement of pure N_2 by GC–TCD.

The Ar+O_2 molar fraction, C_{Ar+O_2}, was obtained based on the calibration line by a least-squares fit of the assigned Ar values in the Ar/He standard mixtures to the measured peak area, because the Ar and O_2 peaks were co-detected by GC–TCD. The Ar molar fraction, C_{Ar}, was then obtained by subtracting the independently measured O_2 molar fraction, C_{O_2}, which was quantified using a galvanic-cell oxygen analyzer:

$$C_{Ar} = C_{Ar+O_2} - 1.13 \times C_{O_2}, \quad (11)$$

where 1.13 is the experimentally determined relative TCD sensitivity factor of O_2 to Ar (Tohjima et al., 2005).

The impurity Ar molar fractions in the pure N_2 used to prepare the HPAs are summarized in Table 3. These molar fractions ranged from 0.046 μmol mol^{-1} to 6.250 μmol mol^{-1}, with associated standard uncertainties ranging from 20 nmol mol^{-1} to 50 nmol mol^{-1}. The molar fractions of impurity O_2 in pure N_2 were between 20 nmol mol^{-1} and 30 nmol mol^{-1}, indicating that the contribution of impurity O_2 to the Ar molar fraction and its uncertainty was negligible.

https://doi.org/10.5194/egusphere-2026-4405
Preprint. Discussion started: 28 September 2026

4.1.2 Determination of molar masses

Application of the IUPAC atomic mass values to the calculation of molar masses resulted in standard uncertainties of 0.18 μmol mol^{-1}, 3.6 μmol mol^{-1}, and 3.7 μmol mol^{-1} for Ar, O_2, and N_2, respectively, which are larger than the target uncertainty of the HPAs. The molar masses (M_i) of the constituents are commonly calculated using the most recent atomic masses reported by the IUPAC. However, the IUPAC atomic masses of Ar, O, and N have relatively large standard uncertainties because they reflect the variability of isotopic abundances in natural terrestrial materials. The isotopic abundances of Ar, O, and N in the HPAs were therefore determined precisely by the conventional mass spectrometry.

An example of the isotopic abundances and their associated standard uncertainties is shown in Table 4. Based on the measured isotopic abundances and the atomic masses of Ar, the molar mass of pure Ar was determined with a relative uncertainty of 0.000038 %. Here, the ^{38}Ar abundance ratio was fixed at the atmospheric value (0.0006289, Böhlk (2014)) because it could not be measured by the mass spectrometer and the pure Ar source gas was derived from atmospheric air. Because ^{36}Ar has a larger mass difference from ^{40}Ar, it has both a greater effect on the molar mass and a higher sensitivity to isotopic fractionation, whereas ^{38}Ar contributes much less because of its lower abundance and smaller mass difference. Given the observed 0.12 % deviation in ^{36}Ar abundance, the deviation in ^{38}Ar abundance is expected to be smaller, and the standard uncertainty of the ^{38}Ar abundance on the molar mass was therefore estimated to be 0.12 %. The ^{38}Ar abundance and its standard uncertainty were estimated to be 0.000629 and 0.000008, respectively. The isotopic abundances of O_2 and N_2 were determined using the same procedure described by Aoki et al. (2019). Based on the measured isotopic abundances and the corresponding atomic masses, the molar masses of pure O_2 and pure N_2 were determined with relative standard uncertainties of 0.000006 % and 0.000029 %, respectively.

Table 4. Isotopic composition and atomic masses of pure oxygen and pure nitrogen used to prepare the highly precise Ar standard mixtures (CPB12763).

Isotope	Atomic mass[a,b]	Isotope abundance		
		Atmosphere[a]	Source gas[a]	Isotopic ratio of source gas[f]
^{14}N	14.0030740074(18)	0.996337(4) [c]	0.996343(4)	
^{15}N	15.000108973(12)	0.003663(4) [c]	0.003657(4)	$\delta^{15}N = (-1.616 \pm 0.001)$ ‰
^{16}O	15.9949146223(25)	0.9975684(9)[d]	0.9975566(9)	
^{17}O	16.99913150(22)	0.0003836(8)[d]	0.0003846(8)	$\delta^{17}O = (2.81 \pm 0.05)$ ‰
^{18}O	17.9991604(9)	0.0020481(5)[d]	0.0020588(5)	$\delta^{18}O = (5.238 \pm 0.003)$ ‰
^{36}Ar	35.967545105(29)	0.0033361(35)[e]	0.003295(4)	$\delta^{36}Ar = (-12.38 \pm 0.05)$ ‰
^{38}Ar	37.96273211(21)	0.0006289(12) [e]	0.000629(8)	
^{40}Ar	39.9623831237(24)	0.9960350(42) [e]	0.996076(5)	

Sources	Atomic mass of nitrogen[a]	Atomic mass of oxygen[a]	Atomic mass of argon[a]
Atmosphere	14.006726(4)	15.999405(1)	39.947798(14)
Source gases	14.006720(4)	15.999427(1)	39.947964(20)

[a] Numbers in parentheses represent the standard uncertainty in the last digits.

[b] Atomic mass and standard uncertainty as determined by De Laeter et al. (2003).

[c] Isotope abundance and standard uncertainty as determined from calculations for the absolute ^{15}N/^{14}N ratio obtained by Junk and Svec (1958).

https://doi.org/10.5194/egusphere-2026-4405
Preprint. Discussion started: 28 September 2026

[d] Isotope abundance and standard uncertainty are calculated using $\delta^{17}O = 12.08$ ‰ and $\delta^{18}O = 23.88$ ‰ vs. VSMOW, as determined by Barkan and Luz (2005). The absolute isotopic ratios for VSMOW and their standard uncertainties were determined by Li et al. (1988) for $^{17}O/^{16}O$ and Baertschi (1976) for $^{18}O/^{16}O$.

[e] Isotope abundance and standard uncertainty are obtained from Böhlk (2014).

[f] The isotopic ratio is defined as the difference from the corresponding atmospheric value (AIST reference air) measured using a mass spectrometer. Numbers following the symbol ± denote the standard uncertainty.

4.1.3 Determination of filling masses

The filling masses of CO_2, Ar, O_2, and N_2 were determined gravimetrically from the cylinder mass differences measured before and after each transfer or filling step. For CO_2 and Ar, the masses were obtained from the mass loss of the 0.9 L cylinders, whereas for O_2 and N_2, they were determined from the mass increase of the 10 L sample cylinder. The 10 L cylinders were weighed using the conventional weighing system.

The transferred and filled masses were calculated using Eqs. (1) – (4). The cylinder masses, m_{cylinder}, used in these calculations were corrected for gas permeation and for buoyancy effects associated with pressure-induced cylinder expansion:

$$m_{\mathrm{cylinder}} = m_{\mathrm{reading}} + \delta m_{\mathrm{permeation}} + \delta m_{\mathrm{buoyancy}} \qquad (12)$$

where m_{reading} is the measured mass reading, and $\delta m_{\mathrm{permeation}}$ and $\delta m_{\mathrm{buoyancy}}$ represent are the corrections for gas permeation and cylinder-expansion-induced buoyancy effects, respectively.

The standard uncertainties of the transferred and filled masses were evaluated by propagating the uncertainties of the individual cylinder mass determinations before and after each transfer or filling step. To quantify these uncertainties, the contributions from (i) mass-reading reproducibility, (ii) gas permeation during weighing, and (iii) buoyancy effects caused by cylinder expansion were evaluated as described in the following sections. The standard uncertainties of the transferred and filled masses were estimated to be 0.049 mg for CO_2 and Ar and 1.2 mg for O_2 and N_2.

Mass readings

The mass of the 0.9 L cylinder was measured using the custom-built weighing system described in Section 2.3.1. To evaluate the reproducibility of the weighing system under conditions representative of actual gas transfer, eleven cooling-cycle experiments were conducted. In each experiment, the sample cylinder was cooled to 1–3 K below the reference cylinder to reproduce the temperature difference that occurs immediately after gas transfer and then weighed. As shown in Fig. 7a, the reproducibility of the mass readings was estimated to be 0.035 mg, expressed as the standard deviation of the average values from the eleven cooling-cycle experiments.

The linearity of the weighing system was evaluated by measuring standard weights ranging from 2 g to 15 g, covering the mass range relevant to the determination of the transferred Ar mass, on the sample−cylinder holder, as shown in Fig. 7b. The measured values were in agreement with the calibration line within their uncertainties, indicating that no significant deviation from linearity was observed.

The 10 L cylinders were weighed using the procedure described in detail by Aoki et al. (2019).

https://doi.org/10.5194/egusphere-2026-4405
Preprint. Discussion started: 28 September 2026

The standard uncertainty of the 0.9 L cylinder mass was estimated to be 0.035 mg and was adopted as the standard uncertainty of the corresponding cylinder mass determinations, whereas for the 10 L cylinders the standard uncertainty was 0.8 mg, as reported by Aoki et al. (2019).

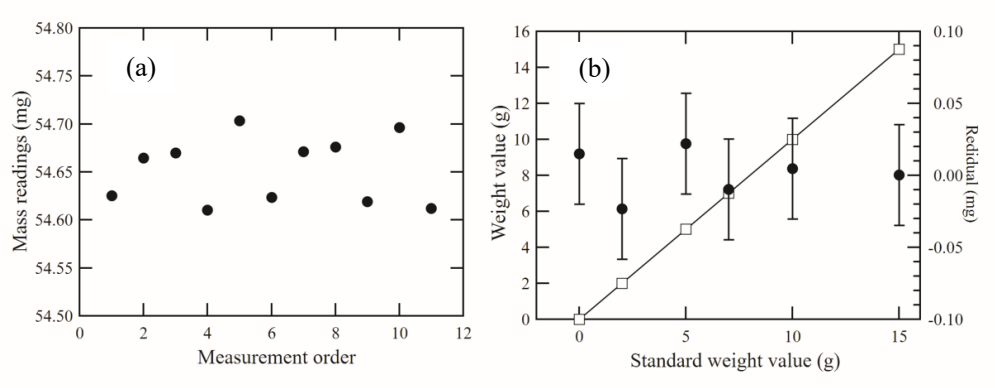

Figure 7. (a) Reproducibility of the mass readings obtained for the sample cylinder after the cylinder had been cooled to 23°C. (b) Calibration line obtained by measuring standard weights of 2 g, 5 g, 7 g, 10 g, and 15 g, and the residuals from the calibration line. Error bars represent the standard uncertainty.

Permeation of source gases during weighing by gas filling

The 0.9 L cylinders used in this study were equipped with diaphragm valves connected by threaded fittings. The valve seals were made of PCTFE, through which gases may slowly permeate (Sturm et al., 2004). Because permeation of pure Ar and CO_2 during weighing could bias the determination of their transferred masses, the extent of permeation was evaluated experimentally by monitoring the mass of a 0.9 L cylinder filled with pure Ar to 1 MPa over a period of four days. Least-squares regression analysis of these data yielded a permeation rate of 2.6 μg day^{-1}. Because weighing of the 0.9 L cylinders was completed within 24 h, the maximum mass loss from permeation was estimated to be only 2.6 μg, which is much smaller than the reproducibility of the weighing system (0.035 mg). The expected permeation loss during weighing was therefore considered negligible, and the contribution of gas permeation was omitted from the uncertainty calculation for the 0.9 L cylinder measurements. For the 10 L cylinders, gas permeation was also considered negligible, as discussed previously by Aoki et al. (2019).

Buoyancy effect of cylinder expansion

For accurate determination of the transferred and filled masses of the source gases, the expansion coefficients of the 0.9 L and 10 L cylinders were determined experimentally. Both cylinders exhibited linear expansion with pressure, as shown in Fig. 4. The observed expansion volumes at 12 MPa were 1.3 mL for the 0.9 L cylinder and 19.5 mL for the 10 L cylinder. Linear regression analysis of the measured data yielded Pearson correlation coefficients of 0.996 for both cylinders, and from these fitted relationships the expansion rates were determined to be 0.109 ± 0.003 mL MPa^{-1} for the 0.9 L cylinder and 1.64 ± 0.06 mL MPa^{-1} for the 10 L cylinder. The number following the symbol ± denotes the standard uncertainty.

The buoyancy effect, $\delta m_{\mathrm{buoyancy}}$, for each source gas was calculated as the product of the cylinder expansion volume, estimated from the filling pressure and the experimentally determined expansion rate, and the density of ambient air. The resulting buoyancy

https://doi.org/10.5194/egusphere-2026-4405
Preprint. Discussion started: 28 September 2026

corrections were 0.005 mg, 0.1 mg, 4 mg, and 14 mg for CO_2, Ar, O_2, and N_2, respectively. Applying these corrections changed the gravimetric Ar molar fraction by −0.08 μmol mol^{-1}.

4.2 Validation of HPAs

To verify the accuracy of the gravimetric preparation, the CO_2 molar fraction and $\delta(O_2/N_2)$ in the HPAs were determined using independently prepared standard mixtures and compared with their gravimetrically assigned values. In contrast, no independently prepared reference gas mixture with a known Ar/N_2 ratio was available for external validation. Therefore, the Ar/N_2 in the HPAs was evaluated based on internal consistency. The CO_2 molar fraction, $\delta(O_2/N_2)$, and $\delta(Ar/N_2)$ values measured in the HPAs are shown in Table 5.

Table 5. $\delta(Ar/N_2)_{HPA\_meas}$ and $\delta(O_2/N_2)_{HPA\_meas}$ calculated using equations (7) and (8); $\delta(^{40}Ar/^{14}N^{14}N)_{HPA\_meas}$ and the CO_2 molar fraction measured by the mass spectrometer and the Picarro G2301; and the differences between $\delta(Ar/N_2)_{HPA\_meas}$ and $\delta(^{40}Ar/^{14}N^{14}N)_{HPA\_meas}$. For each cylinder, the upper and lower rows give the values from the conventional and new mass spectrometers, respectively.

Cylinder number	$\delta(Ar/N_2)_{HPA\_meas}$	$\delta(^{40}Ar/^{14}N_2)_{HPA\_meas}$	$\delta(Ar/N_2)_{HPA\_meas} - \delta(^{40}Ar/^{14}N_2)_{HPA\_meas}$	$\delta(O_2/N_2)_{HPA\_meas}$	CO_2 molar fraction
CPB12763	335.6 ± 6.5	364.8 ± 6.5	−29.2	−690.0 ± 3.2	410.09 ± 0.05
	340.3 ± 6.5	369.3 ± 6.5	−29.0	−699.6 ± 3.2	
CPB16187	4414.5 ± 6.5	4444.2 ± 6.5	−29.7	−1409.5 ± 3.2	401.70 ± 0.05
	4387.6 ± 6.5	4417.1 ± 6.5	−29.5	−1414.1 ± 3.2	
CPB16370	−1971.1 ± 6.5	−1942.0 ± 6.5	−29.1	−1888.4 ± 3.2	421.01 ± 0.05
	−1973.0 ± 6.5	−1944.2 ± 6.5	−28.8	−1902.9 ± 3.2	
CPB31357	2207.5 ± 6.5	2236.8 ± 6.5	−29.3	679.0 ± 3.2	394.38 ± 0.05
	2202.5 ± 6.5	2231.6 ± 6.5	−29.1	685.1 ± 3.2	
CPB16246	−89.8 ± 6.5	−60.7 ± 6.5	−29.1	3331.7 ± 3.2	430.16 ± 0.05
	−87.2 ± 6.5	−58.4 ± 6.5	−28.8	3339.3 ± 3.2	
CPC00484	−10649.9 ± 6.5	−10621.5 ± 6.5	−28.4	−7159.3 ± 3.2	438.47 ± 0.05
	−10669.3 ± 6.5	−10641.1 ± 6.5	−28.2	−7185.6 ± 3.2	
CPB28571	−1126.1 ± 6.5	−1103.0 ± 6.5	−23.1	3110.8 ± 3.2	409.93 ± 0.05
	−1104.3 ± 6.5	−1081.2 ± 6.5	−23.1	3121.0 ± 3.2	
CPC00486	−5120.8 ± 6.5	−5097.9 ± 6.5	−22.9	−1910.3 ± 3.2	450.94 ± 0.05
	−5106.4 ± 6.5	−5083.5 ± 6.5	−22.9	−1915.3 ± 3.2	

For $\delta(Ar/N_2)_{HPA\_meas}$, $\delta(O_2/N_2)_{HPA\_meas}$, and $\delta(^{40}Ar/^{14}N^{14}N)_{HPA\_meas}$, the top row gives the measured values on the EMRI/AIST scale using the conventional mass spectrometer, and the bottom row gives the results using the new mass spectrometer; all are given in per meg. CO_2 molar fractions were measured by the Picarro G2301. Values for $\delta(Ar/N_2)_{HPA\_meas}$, $\delta(O_2/N_2)_{HPA\_meas}$, and $\delta(^{40}Ar/^{14}N^{14}N)_{HPA\_meas}$, and for CO_2 are given in per meg. Numbers following the symbol ± denote the standard uncertainty.

https://doi.org/10.5194/egusphere-2026-4405
Preprint. Discussion started: 28 September 2026

4.2.1 CO_2 validation

The CO_2 molar fractions determined using the Picarro G2301 agreed well with the gravimetrically assigned values, as shown in Fig. 8(a). The differences between the measured and assigned values ranged from −0.05 μmol mol^{-1} to 0.06 μmol mol^{-1}, which

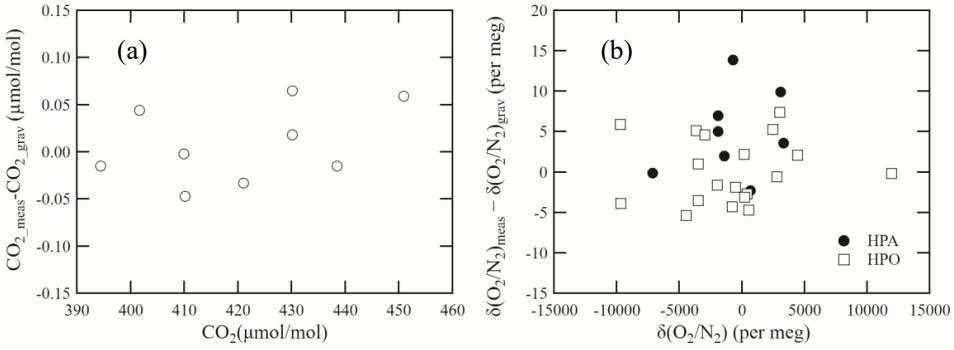

Figure 8. (a) Differences between the measured and gravimetric CO_2 molar fractions, and (b) residuals of $\delta(O_2/N_2)$ in the HPAs and HPOs from the $\delta(O_2/N_2)$ values on the EMRI/AIST scale.

are within the expanded uncertainties (k = 2) of the gravimetric preparation and the analytical measurements. These results demonstrate that the gravimetrically assigned CO_2 molar fractions are consistent with the independent measurements within the combined standard uncertainties.

4.2.2 O_2/N_2 validation

The determined $\delta(O_2/N_2)$ values were compared with those of the HPOs using the conventional mass spectrometer (Fig. 8b). The measurements were performed relative to the reference air on the EMRI/AIST scale, which is natural air contained in a 48 L aluminum cylinder with a diaphragm valve (Ishidoya and Murayama, 2014). The differences ranged from −2.3 per meg to 13.9 per meg. Except for one sample (CPB16246), all HPAs agreed with the EMRI/AIST scale within the expanded uncertainty (k = 2) of 10.5 per meg, calculated from the combined uncertainties of the gravimetric preparation and the measurement. Even for CPB16246, the deviation was only slightly larger than the expanded uncertainty. Overall, these results indicate good agreement between the HPA and HPO preparation methods.

4.2.3 Ar/N_2 ratio

Figure 9 shows the relationship between the gravimetrically assigned $\delta(Ar/N_2)$ values and those measured using the new and conventional mass spectrometers. Excellent linear agreement was observed for both systems, and the fitted slopes from least-squares analysis were 1.00178 ± 0.00070 and 1.00196 ± 0.00070, respectively. The two values agreed within their uncertainties. The residuals ranged from −10.5 per meg to 16.6 per meg for the new mass spectrometer and from −8.8 per meg to 18.0 per meg for the conventional mass spectrometer. Their standard uncertainties, which combine the uncertainties of the measured and gravimetric values, ranged from 8.1 per meg to 8.8 per meg. Unlike for CO_2 and O_2/N_2, no independent reference standard was available to validate the Ar/N_2 ratio. The consistency of the assigned Ar/N_2 values was therefore evaluated using the residuals of the least-squares fits relating the gravimetrically assigned values to the measured values. Although a few residuals exceed the corresponding expanded uncertainty (Fig. 9(b)), no systematic difference was observed between the residuals from the new and

https://doi.org/10.5194/egusphere-2026-4405
Preprint. Discussion started: 28 September 2026

conventional mass spectrometers. The residuals were comparable to the combined standard uncertainties, indicating good agreement between the gravimetrically assigned values and the analytical response.

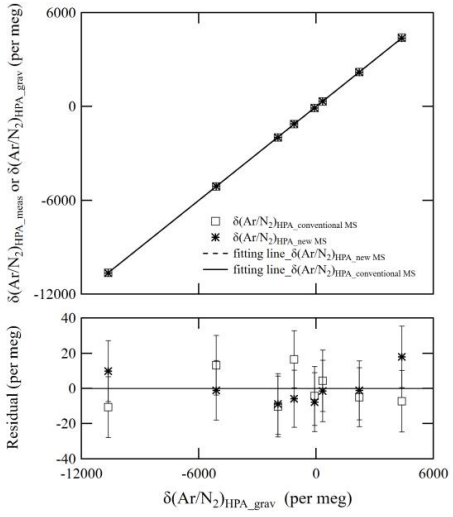

Figure 9. (a) Relationship between $\delta(Ar/N_2)_{HPA\_grav}$ and $\delta(Ar/N_2)_{HPA\_meas}$ on the EMRI/AIST scale. (b) Residuals of the fit to $\delta(Ar/N_2)_{HPA\_meas}$. Error bars represent the expanded uncertainty (k = 2).

Overall, the gravimetrically assigned CO_2 molar fractions and O_2/N_2 ratios were independently validated against established reference scales. Although no independent reference standard was available for Ar/N_2, the observed calibration residuals were comparable to the combined standard uncertainties, indicating good internal consistency of the assigned Ar/N_2 values. Together, these results support the validity of the gravimetric preparation procedure and the associated uncertainty estimates for the HPAs.

4.3 Application of HPAs to the determination of the absolute atmospheric Ar/N_2 ratio and Ar molar fraction

To demonstrate the applicability of the validated HPAs, the absolute Ar/N_2 ratio of the AIST reference air was first redetermined. The resulting calibration was then applied to atmospheric observations at Hateruma Island and Cape Ochiishi to derive the absolute atmospheric Ar/N_2 ratio and Ar molar fraction. In the following section, the number following the symbol ± represents the standard uncertainty.

4.3.1 Redetermining the absolute Ar/N_2 ratio in AIST reference air

The absolute Ar/N_2 ratio of the AIST reference air was redetermined from the line obtained by least-squares regression between the gravimetrically assigned Ar/N_2 values of the HPAs and the corresponding measured $\delta(Ar/N_2)$ values on the EMRI/AIST scale. The resulting value was 0.01195567 ± 0.00000011, compared with the previously reported value of 0.0119542 ± 0.0000009. The redetermined value reduced the associated standard uncertainty by approximately a factor of 8. The two values agreed within their expanded uncertainty (k = 2). This result further supports the consistency between the gravimetric preparation of the HPAs and the previous EMRI/AIST scale.

https://doi.org/10.5194/egusphere-2026-4405
Preprint. Discussion started: 28 September 2026

4.3.2 Atmospheric absolute Ar/N_2 ratios and Ar molar fractions

The validated HPAs were applied to determine the absolute atmospheric Ar/N_2 ratios and Ar molar fractions using air samples collected between January and December 2021 at Hateruma Island and Cape Ochiishi, Japan. Because atmospheric Ar/N_2 exhibits seasonal variability, the value derived here should be regarded as the annual mean atmospheric composition for 2021 rather than a universal atmospheric constant.

The annual mean $\delta(Ar/N_2)$ and $\delta(O_2/N_2)$ derived from the air sample measurements were −58.8 per meg and −214 per meg, respectively. Using the $(Ar/N_2)_{ref}$ and $(O_2/N_2)_{ref}$ ratios for the AIST reference air, the corresponding absolute Ar/N_2 and O_2/N_2 ratios were 0.01195497 ± 0.00000013 and 0.2680355 ± 0.0000018, respectively. The Ar molar fraction, x_{Ar}, was then calculated from the Ar/N_2 ratio using

$$x_{Ar} = K \times \frac{Ar/N_2}{(1+O_2/N_2+Ar/N_2)} \quad (13)$$

where K is the sum of the molar fractions of N_2, O_2, and Ar in dry air and was estimated to be 999552.8 ± 0.1 μmol mol^{-1}. This value was obtained by subtracting the molar fractions of the minor atmospheric constituents. The minor constituents considered were Ne (18.18 μmol mol^{-1}), He (5.24 μmol mol^{-1}), Kr (1.14 μmol mol^{-1}), H_2 (0.52 μmol mol^{-1}), CO (0.15 μmol mol^{-1}), and Xe

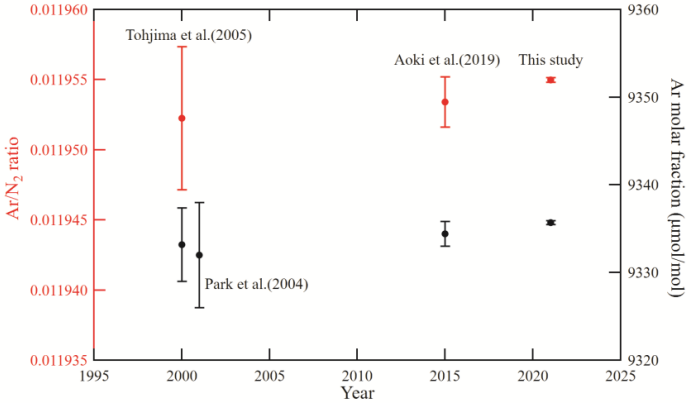

Figure 10. Atmospheric Ar molar fractions and their expanded uncertainties reported in previous studies and in the present work. Error bars represent the expanded uncertainties (k = 2).

(0.09 μmol mol^{-1}), reported by Tohjima et al. (2005), together with CO_2 (418.8 μmol mol^{-1}), CH_4 (1.91 μmol mol^{-1}), and N_2O (0.34 μmol mol^{-1}). The CO_2 molar fraction was the average value in the air samples measured using the conventional mass spectrometer. The CH_4 and N_2O molar fractions were the global annual means for 2021 reported by the WMO (2021). The corresponding atmospheric Ar molar fraction was determined to be 9335.71 ± 0.10 μmol mol^{-1}. It should be noted that the reported standard uncertainties do not account for seasonal variations in atmospheric composition; the variability observed in atmospheric measurements may therefore exceed the uncertainties estimated in this study.

Aoki et al. (2019) reported an Ar/N_2 ratio of 0.0119534 ± 0.0000009, corresponding to an Ar molar fraction of 9334.4 ± 0.7 μmol mol^{-1}. Tohjima et al. (2005) and Park et al. (2004) reported Ar molar fractions of 9333.2 ± 2.1 μmol mol^{-1} and 9332 ± 3 μmol mol^{-1}, respectively. The atmospheric Ar/N_2 ratio and Ar molar fraction determined in this study were slightly higher than these previously reported values, but all estimates remain consistent within their expanded uncertainties (Fig. 10).

https://doi.org/10.5194/egusphere-2026-4405
Preprint. Discussion started: 28 September 2026

5 Discussion

5.1 Reduction of uncertainty in Ar/N_2 standards

The standard uncertainty of the Ar molar fraction in the HPAs was reduced by more than an order of magnitude relative to that of the previously developed HPOs. The uncertainty budget analysis (Table 2) indicates that the dominant contributions arise from the determination of the source-gas masses and the purity of the source gases, whereas the contribution from the molar masses was negligible.

Relative to the HPOs reported by Aoki et al. (2019), the uncertainty contributions from the source-gas masses and molar masses were reduced by factors of approximately 13 and 60, respectively, whereas the contribution from gas purity remained largely unchanged, even though the molar fraction of impurity Ar in pure N_2 differed by nearly a factor of 20 among the individual N_2 cylinders. These reductions demonstrate that the improved preparation procedure eliminated the major sources of uncertainty associated with the determination of the transfer and filling masses and the molar masses of the source gases. A more detailed analysis showed that the determination of the transferred Ar mass and the quantification of trace Ar impurities in pure N_2 are now the principal factors limiting the overall uncertainty of the Ar molar fraction. Further reductions in uncertainty will therefore depend largely on more accurate determination of the transferred Ar mass and quantification of trace Ar impurities in N_2.

Because independent primary standard mixtures for Ar/N_2 are not currently available, validation of the assigned Ar/N_2 values relied on the internal consistency between the gravimetric assignments and the calibration measurements. Nevertheless, because the independent validation of the CO_2 molar fractions and O_2/N_2 ratios indicated that the CO_2, O_2, and N_2 molar fractions were correct, the absence of systematic residuals in the Ar/N_2 calibration provides indirect but strong evidence that no significant bias remains in the assigned Ar/N_2 values.

The resulting standard uncertainty of the HPAs (4.8 per meg – 5.9 per meg in δ(Ar/N_2)) is comparable to or smaller than that of current measurement systems. This level of performance enables the use of HPAs as primary standards for high-precision atmospheric observations and provides a basis for improving consistency among atmospheric observation networks through traceable Ar/N_2 calibration.

5.2 Effect of compositional changes during CO_2/Ar transfer

The observed lot-to-lot discrepancies indicate that gravimetric uncertainty estimates alone are insufficient. In the initial preparation approach, the discrepancies in δ(Ar/N_2) were substantially larger than the long-term atmospheric Ar/N_2 trends of 0.75 per meg yr^{-1} and 0.89 per meg yr^{-1} reported by Ishidoya et al. (2021), confirming that even small transfer-induced fractionation effects can severely compromise the accuracy of the HPAs.

Previous studies have shown that gas composition can change during cylinder-to-cylinder transfer owing to thermal-diffusion fractionation (Aoki et al., 2022, 2025). Consistent with these findings, cylinder-to-cylinder transfer experiments using CO_2/Ar mixtures in a 10 L cylinder revealed a decrease of approximately 0.04 % in the CO_2/Ar ratio due to thermal fractionation. Such compositional changes in the CO_2/Ar mixture correspond to deviations of several tens of per meg in δ(Ar/N_2). Similar compositional changes are expected during transfer from the 0.9 L cylinder to another cylinder, where thermal fractionation may also occur. Although the magnitude of this effect was not quantified in the present study, these effects were considered the primary causes of the observed discrepancy. The improved preparation procedure avoids this problem by introducing pure CO_2, Ar, O_2, and N_2 independently into the final cylinder. The agreement between the gravimetrically assigned and independently measured values confirms that this approach effectively suppresses transfer-induced compositional bias.

https://doi.org/10.5194/egusphere-2026-4405
Preprint. Discussion started: 28 September 2026

5.3 Importance of Ar impurity and isotopic composition

As the uncertainty of Ar molar fraction in the HPAs was reduced to the per meg level, factors that had been negligible in previous HPO preparations became increasingly important. In the HPOs, the uncertainty in the Ar molar fraction was dominated by the determination of the Ar mass and the molar mass of Ar. In contrast, trace Ar impurities in the source N_2 emerged as a major contributor to the uncertainty at the level achieved in this study. These findings indicate that further improvements in Ar/N_2 standards will require the characterization of impurities at levels previously considered negligible.

Another important factor is the isotopic composition of the source gases. The molar masses used in the gravimetric calculations were derived directly from the measured isotopic abundances of Ar, O, and N. Although the source gases were obtained from the same suppliers and purity grades as those used by Aoki et al. (2019), the atomic masses derived from the measured isotopic abundances differed slightly from the previously adopted values. These differences resulted in changes of −0.02 μmol mol^{-1}, +0.92 μmol mol^{-1}, and −0.91 μmol mol^{-1} in the assigned Ar, O_2, and N_2 molar fractions, respectively. Despite these shifts, the contribution of the molar masses to the uncertainty of the Ar molar fraction remained negligible because the isotopic abundances were determined with high precision. Nevertheless, the observed differences demonstrate that direct determination of the isotopic abundances is important for achieving highly accurate gravimetric standards.

The isotopic compositions of the source gases also influence the interpretation of Ar/N_2 measurements. Because these compositions differed from those of atmospheric air, the measured $\delta(^{40}Ar/^{14}N^{14}N)$ values differed systematically from the corresponding total $\delta(Ar/N_2)$ values by approximately 23 per meg – 30 per meg. This offset is substantially larger than the uncertainty of the gravimetrically assigned $\delta(Ar/N_2)$ and therefore cannot be neglected. These results demonstrate that total Ar/N_2 ratios, rather than the isotope-specific $^{40}Ar/^{14}N^{14}N$ ratios, should be used when assigning Ar/N_2 values with HPAs. Failure to account for differences in isotopic composition would introduce a systematic bias comparable to several decades of the long-term atmospheric Ar/N_2 trend reported by Ishidoya et al. (2021). This offset of 23 per meg – 30 per meg is substantially larger than the uncertainty of the HPAs and demonstrates that accurate characterization of the isotopic composition is essential for establishing traceable absolute Ar/N_2 scales.

5.4 Implications for atmospheric observations

The present study establishes an absolute Ar/N_2 calibration framework with substantially reduced uncertainty, an approximately tenfold improvement over the previous value. The redetermined absolute Ar/N_2 ratio of the AIST reference air enabled a corresponding revision of atmospheric Ar/N_2 values.

The atmospheric $\delta(Ar/N_2)$ in 2021 was slightly higher than that in 2015, the difference corresponding to approximately 4 per meg in $\delta(Ar/N_2)$. Although this difference is smaller than the standard uncertainty and therefore does not provide statistically significant evidence for an increase in atmospheric Ar/N_2, its magnitude is consistent with that expected from the reported long-term trend (Ishidoya et al., 2021).

The Ar molar fraction in 2015 reported by Aoki et al. (2019) was recalculated as 9335.51 ± 0.10 μmol mol^{-1} on the redetermined EMRI/AIST scale, indicating that the atmospheric Ar molar fraction increased by 0.20 μmol mol^{-1} from 2015 to 2021. However, this increase does not directly represent a change in the absolute abundance of atmospheric Ar, because molar fractions are also affected by variations in the total abundance of other atmospheric constituents, particularly O_2 and CO_2. The absolute Ar/N_2 ratio therefore provides a more robust metric than the Ar molar fraction for detecting long-term changes associated with oceanic and atmospheric processes.

https://doi.org/10.5194/egusphere-2026-4405
Preprint. Discussion started: 28 September 2026

Assuming that the atmospheric Ar/N_2 trend reported by Ishidoya et al. (2021) continues, the cumulative change would reach approximately 23 per meg – 27 per meg over a 30-year period. Such changes are substantially larger than the uncertainty of the absolute Ar/N_2 framework developed in this study. These results indicate that absolute Ar/N_2 measurements have the potential to detect multidecadal changes associated with ocean heat uptake.

Because maintaining the scale of Ar/N_2 reference air over several decades is inherently challenging, a traceable absolute Ar/N_2 framework provides a robust basis for long-term atmospheric monitoring. The HPAs developed in this study therefore establish a foundation for the future use of atmospheric Ar/N_2 as an independent tracer of OHC and climate change.

6 Conclusion

A gravimetric preparation method was developed for highly precise Ar standard mixtures (HPAs) composed of ambient-level CO_2, Ar, O_2, and N_2 for atmospheric Ar/N_2 measurements. The procedure was improved by introducing pure CO_2, Ar, O_2, and N_2 independently and by determining the transferred Ar mass from the mass loss of a 0.9 L cylinder using a newly developed high-precision weighing system. In addition, the isotopic abundances and trace Ar impurities in the source gases were incorporated into the gravimetric calculations to achieve the target uncertainty.

Eight HPAs were prepared and independently evaluated. The measured CO_2 mole fractions and O_2/N_2 ratios agreed with the gravimetrically assigned values within their combined uncertainties, and the Ar/N_2 calibration residuals were consistent with the estimated uncertainty. These results demonstrate the validity of the gravimetric assignments and the associated uncertainty estimates.

The resulting standard uncertainty of the Ar/N_2 ratio was reduced to approximately 5 per meg, corresponding to about 0.05 μmol mol^{-1} in the Ar mole fraction and more than an order of magnitude smaller than that of the previously developed HPOs. Using the developed HPAs, the absolute Ar/N_2 ratio of the AIST reference air was redetermined as $0.01195567 \pm 0.000000011$, a 8-fold reduction in uncertainty. Application of the revised calibration to atmospheric observations yielded an atmospheric Ar/N_2 ratio of $0.01195497 \pm 0.00000013$ and an atmospheric Ar mole fraction of 9335.71 ± 0.10 μmol mol^{-1} for 2021.

The developed HPAs establish a metrologically traceable framework for absolute atmospheric Ar/N_2 measurements. This framework reduces dependence on the long-term maintenance of reference-air scales and provides a foundation for future applications of atmospheric Ar/N_2 as an independent tracer of ocean heat uptake and climate change.

Data availability

The data presented in this article are available upon request by email (Nobuyuki Aoki; aoki-nobu@aist.go.jp).

Author contributions

NA designed the study, performed the experiments, and prepared the first draft of the manuscript. SI performed the mass spectrometry measurements. NM carried out the impurity analyses of the pure CO_2. All authors contributed to the interpretation of the results and to the final version of the manuscript.

Competing interests

The contact author has declared that none of the authors has any competing interests.

Acknowledgments

https://doi.org/10.5194/egusphere-2026-4405
Preprint. Discussion started: 28 September 2026

We thank Yasunori Tohjima and Yukio Terao of the National Institute for Environmental Studies for their valuable assistance in collecting air samples at Hateruma Island and Cape Ochiishi.

Financial support

This study was supported in part by JSPS KAKENHI (grant nos. 22H05006 and 26K03079) and the Global Environment Research Coordination System of the Ministry of the Environment, Japan (grant nos. METI1454 and METI1953).

References

Abraham, J. P., Baringer, M., Bindoff, N. L., Boyer, T., Cheng, L. J., Church, J. A., Conroy, J. L., Domingues, C. M., Fasullo, J. T., Gilson, J., Goni, G., Good, S. A., Gorman, J. M., Gouretski, V., Ishii, M., Johnson, G. C., Kizu, S., Lyman, J. M., Macdonald, A. M., Minkowycz, W. J., Moffitt, S. E., Palmer, M. D., Piola, A. R., Reseghetti, F., Schuckmann, K., Trenberth, K. E., Velicogna, I., and Willis, J. K.: A review of global ocean temperature observations: Implications for ocean heat content estimates and climate change, Rev. Geophys., 51, 450–483, https://doi.org/10.1002/rog.20022, 2013.

Aoki, N., Ishidoya, S., Matsumoto, N., Watanabe, T., Shimosaka, T., and Murayama, S.: Preparation of primary standard mixtures for atmospheric oxygen measurements with less than 1 μmolmol^{-1} uncertainty for oxygen molar fractions, Atmos. Meas. Tech., 12, 2631–2646, https://doi.org/10.5194/amt-12-2631-2019, 2019.

Aoki, N., Ishidoya, S., Murayama, S., and Matsumoto, N.: Influence of CO_2 adsorption on cylinders and fractionation of CO_2 and air during the preparation of a standard mixture, Atmos. Meas. Tech., 15, 5969–5983, https://doi.org/10.5194/amt-15-5969-2022, 2022.

Aoki, N., Ishidoya, S., Murayama, S., and Matsumoto, N.: CO_2 deviation in a cylinder due to consumption of a standard gas mixture, Atmos. Meas. Tech., 18, 6053–6067, https://doi.org/10.5194/amt-18-6053-2025, 2025

Alink, A. and van der Veen, A. M. H.: Uncertainty calculations for the preparation of primary gas mixtures: I. Gravimetry, Metrologia, 37 641−650, 2000

Baertschi, P.: Absolute ^{18}O content of standard mean ocean water, Earth Planet. Sci. Lett., 31, 341–344, 1976.

Barkan, E. and Luz, B.: High precision measurements of $^{17}O/^{16}O$ and $^{18}O/^{16}O$ ratios in H_2O, Rapid Commun. Mass Spectrom., 19, 3737–3742, 2005.

Blaine, T. W.: Continuous measurements of atmospheric ar gon/nitrogen as a tracer of air-sea heat flux: Models, methods, and data, PhD thesis, University of California, San Diego, La Jolla, USA, 2005.

Böhlk, J. K.: Variation in the terrestrial isotopic composition and atomic weight of argon (IUPAC Technical Report), Pure Appl. Chem., 86, 1421−1432, 2014.

Cassar, N., Mckinley, G. A., Bender, M. L., Mika, R., and Battle, M.: An improved comparison of atmospheric Ar/N_2 time series and paired ocean-atmosphere model predictions, J. Geophys. Res., 113, D21122, https://doi.org/10.1029/2008JD009817, 2008.

Cheng, L., Abraham, J., Hausfather, Z., and Trenberth, K. E.:How fast are the oceans warming?, Science, 363, 128–129, https://doi.org/10.1126/science.aav7619, 2019.

De Laeter, J. R., Böhlke, J. K., De Bièfre, P., Hidaka, H., Peiser, H. S., Rosman, K. J. R., and Taylor P. D. P.: Atomic weights of the elements: Review 2000 (IUPAC Technical Report), Pure Appl. Chem., 75, 683–800, 2003.

Ishidoya, S., and Murayama, S.: Development of a new high precision continuous measuring system for atmospheric O_2/N_2 and Ar/N_2 and its application to the observation in Tsukuba, Japan, Tellus B: Chem. Phys. Meteorol., 66, 22574, 2014.

https://doi.org/10.5194/egusphere-2026-4405
Preprint. Discussion started: 28 September 2026

Ishidoya, S., Sugawara, S., Tohjima, Y., Goto, D., Ishijima, K., Niwa, Y., Aoki, N., and Murayama, S.: Secular change in atmospheric Ar/N_2 and its implications for ocean heat uptake and Brewer–Dobson circulation, Atmos. Chem. Phys, 21, 1357–1373, 2021, https://doi.org/10.5194/amt-14-6181-2021.

ISO 6142-1:2015, Gas Analysis-Preparation of Calibration Gas Mixtures-Part 1: Gravimetric Method for Class I Mixtures, International Organization for Standardization, ISO 6142–1:2015.

ISO 6145-7: Gas analysis– Preparation of calibration gas mixtures using dynamic methods–Part 7: Thermal mass-flow, available at: https://www.iso.org/standard/45471.html (last access: January 2023), 2018.

Junk, G. A., and Svec, H. J.: The absolute abundance of the nitrogen isotopes in the atmosphere and compressed gas from various sources, Geochim. Cosmochim. Acta, 14, 234–243, 1958.

Keeling, R. F., and Shertz, S. R.: Seasonal and interannual variations in atmospheric oxygen and implications for the global carbon cycle. Nature, 358, 723–727, 1992.

Keeling, R. F., Blaine, T. Paplawsky, B, Katz, L., Atwood, C., and Brockwell, T.: Measurement of changes in atmospheric Ar/N_2 ratio using a rapid-switching, single-capillary mass spectrometer system, Tellus 56 B, 322-338, 2004

Li, W., Ni, B., Jin, D., and Chang, T. L.: Measurement of the absolute abundance of oxygen–17 in V–SMOW, Kexue Tnbao, 33, 1610–1613, 1988.

Matsumoto, N., Watanabe, T., Maruyama, M., Horimoto, Y., Maeda, T., and Kato, K.: Development of mass measurement equipment using an electronic mass-comparator for gravimetric preparation of reference gas mixtures, Metrologia, 41, 178–188, 2004.

Milton, M. J. T., Vargha, G. M., and Brown, A. S.: Gravimetric methods for the preparation of standard gas mixtures, Metrologia, 48, R1–R9, 2011.

Oh, S. H., Kim, B. M., and Kang, N.: Evaluation of changes in cylinder volume due to gas filling and subsequent release, Metrologia, 50, 318–324, 2013.

Park, S. Y., Kim, J. S., Lee, J. B., Esler, M. B., Davis, R. S., and Wielgosz, R. I.: A redetermination of the argon content of air for buoyancy corrections in mass standard comparisons, Metrologia, 41, 387–395, 2004.

Rhein, M., RintoulS., Aoki, S., Campos, E., Chambers, D., Feely, R., Gulev, S., Johnson, G., Josey, S., Kostianoy, A., Mauritzen, C., Roemmich, D., Talley, L., and Wang, F.: Chapter 3: Observations: Ocean, in: Climate Change 2013: The Physical Science Basis. Contribution of Working Group I to the Fifth Assessment Report of the Intergovernmental Panel on Climate Change, edited by: Stocker, T., Qin, D., Plattner, G.-K., Tignor, M., Allen, S., Boschung, J., Nauels, A., Xia, Y., Bex, V., and Midgley, P., Cambridge University Press, Cambridge University Press, Cambridge, United Kingdom and New York, USA, 2013.

Sturm, P., Leuenberger, M., Sirignano, C., Neubert, R. E. M., Meiger, H. A. J., Langenfelds, R., Brand, W. A., and Tohjima, Y.: Permeation of atmospheric gases through polymer O-rings used in flasks for air sampling, J. Geophys. Res., 109, D04309, 2004.

von Schuckmann, K., Cheng, L., Palmer, M. D., Hansen, J., Tassone, C., Aich, V., Adusumilli, S., Beltrami, H., Boyer,T., Cuesta-Valero, F. J., Desbruyères, D., Domingues, C., García-García, A., Gentine, P., Gilson, J., Gorfer, M., Haimberger, L., Ishii, M., Johnson, G. C., Killick, R., King, B. A., Kirchengast, G., Kolodziejczyk, N., Lyman, J., Marzeion,B., Mayer, M., Monier, M., Monselesan, D. P., Purkey, S., Roemmich, D., Schweiger, A., Seneviratne, S. I., Shepherd, A., Slater, D. A., Steiner, A. K., Straneo, F., Timmermans, M.-L., and Wijffels, S. E.: Heat stored in the Earth system: Where does the energy go?, Earth Syst. Sci. Data, 12, 2013–2041, https://doi.org/10.5194/essd-12-2013-2020, 2020

von Schuckmann, K., Minière, A., Gues, F., Cuesta-Valero, F. J., Kirchengast, G., Adusumilli, S., Straneo, F., Ablain, M., Allan, R. P., Barker, P. M., Beltrami, H., Blazquez, A., Boyer, T., Cheng, L., Church, J., Desbruyeres, D., Dolman, H., Domingues,

https://doi.org/10.5194/egusphere-2026-4405
Preprint. Discussion started: 28 September 2026

C. M., García-García, A., Giglio, D., Gilson, J. E., Gorfer, M., Haimberger, L., Hakuba, M. Z., Hendricks, S., Hosoda, S., Johnson, G. C., Killick, R., King, B., Kolodziejczyk, N., Korosov, A., Krinner, G., Kuusela, M., Landerer, F. W., Langer, M., Lavergne, T., Lawrence, I., Li, Y., Lyman, J., Marti, F., Marzeion, B., Mayer, M., MacDougall, A. H., McDougall, T., Monselesan, D. P., Nitzbon, J., Otosaka, I., Peng, J., Purkey, S., Roemmich, D., Sato, K., Sato, K., Savita, A., Schweiger, A., Shepherd, A., Seneviratne, S. I., Simons, L., Slater, D. A., Slater, T., Steiner, A. K., Suga, T., Szekely, T., Thiery, W., Timmermans, M.-L., Vanderkelen, I., Wjiffels, S. E., Wu, T., and Zemp, M.: Heat stored in the Earth system 1960–2020: Where does the energy go?, Earth Syst. Sci. Data, 15, 1675–1709, https://doi.org/10.5194/essd-15-1675-2023, 2023.

Tohjima, Y.: Method for measuring changes in the atmospheric O_2/N_2 ratio by a gas chromatograph equipped with a thermal conductivity detector, J. Geophys. Res., 105, 14575–14584, 2000.

Tohjima, Y., Machida, T., Watai, T., Akama, I., Amari, T., and Moriwaki, Y.: Preparation of gravimetric standards for measurements of atmospheric oxygen and reevaluation of atmospheric oxygen concentration, J. Geophys. Res., 110, D1130, 2005.